

Investigating landscape resistance using a connectivity modelling method

Romain Cottet

(16-605-175)

Supervisor: Dr. Janine Bolliger

Swiss Federal Institute for Forest, Snow and Landscape Research (WSL),

Landscape Dynamics

Co-supervisor: Dr. Peter Bach

Swiss Federal Institute of Aquatic Science and Technology (EAWAG),

Department Urban Water Management

Advisor: Dr. Julia Donati

Swiss Federal Institute for Forest, Snow and Landscape Research (WSL),

Landscape Dynamics

Swiss Federal Institute of Aquatic Science and Technology (EAWAG),

Department Urban Water Management

Master's thesis

Master's degree programme in Environmental Sciences

April 6, 2021

Contents

List of Figures

List of Tables

Acknowledgements

I would like to thank Janine Bolliger and Peter Bach for their precious advice and comments on this thesis. I would also like to thank them for the time spent helping me get a better understanding of the whole method and results.

I also want to thank Giulia Donati, Max Maurer, Sven Eggimann, Achilleas Psomas, Lucie Roth and Philipp Lischer for the fruitful discussions during our weekly meetings.

Thank you as well to Robert Pazûr for kindly sharing his data on Swiss cropland and grassland and to Giulia and Lucie for the bits and pieces of code they shared.

A special thanks to Lucie for her kind ear and patient answers to all my questions.

Thanks to my sister Pauline for taking time on a sunny Sunday to give an external view on this work.

Finally, I would like to thank my flatmates for the joyful latino evenings to clear the day and for feeding me nice food during the quarantine I fruitfully used to work on this thesis.

Abstract

The concept of blue-green infrastructure has been put forward as a tool to preserve biodiversity and ecosystem services from detrimental human activities and allow cohabitation. Among the different factors determining the efficiency of those infrastructures, their connectivity has been found to be of major importance. Many models have been created to assess the capacity of the landscape to favor or hinder movement of species. Among those, Circuitscape has been widely used in ecology and other fields. However, the resistance surfaces used as input by the software have sometimes been criticised because of the partly subjective knowledge included in estimating them. By applying an existing resistance modelling method to a network representing the landscape, I could explore numerous resistance models for various variables and investigate the role they played for connectivity. Five Swiss amphibian species were used as case study species. I found that the determinant variable underlying landscape connectivity were specific to each species. I could nonetheless identify the shortest distance to water and the slope to be dominant factors, closely followed by the traffic. The land-cover appeared to be a poor predictor of landscape connectivity due to a loss of information when transposing the data to the network. These results illustrate the crucial importance of carefully modelling resistance when carrying out a connectivity analysis and show how much can be learned about the role of the different variables for connectivity in the process. Overall, this study makes a strong case for the opportunities of the method for connectivity modelling in a blue-green infrastructure context.

Chapter 1

Introduction

Biodiversity has been put under immense pressure by the development of human activities in the last decades. In a world where the surface of untouched land decreases everyday, the concept of blue-green infrastructure emerged to acknowledge the importance of maintaining environments where ecological processes can thrive for their own good and for the good of humanity (Reid et al. 2005). It postulates that in order for those processes to cohabit with human activities, suitable areas combining both terrestrial and aquatic environments need to be preserved especially in human dominated landscapes such as cities. It has become increasingly clear that not only do those areas need to be of suitable size and quality, they need to be ecologically interconnected as well for those processes to be maintained at all scales in the long term (eg. Rosenberg et al. 1997; Cushman 2006).

A broad range of methods is available to quantify ecological connectivity across landscapes (eg. Bar-David et al. 2007; Schulte et al. 2007; Rayfield, Fortin, et al. 2010; Luqman et al. 2018). Among those the combination of electrical circuit theory and random walk theory proposed by Brad H. McRae et al. (2008) hypothesizes that the movement of individuals or species across the landscape at different scales can be approximated by the distribution of the current in a circuit of resistances representing that specific landscape. The software Circuitscape has been extensively used to produce connectivity maps in order to inform conservation decisions to maintain these blue-green infrastructures (eg. Rae et al. 2007; Rayfield, Pelletier, et al. 2016). Assuming that individual environmental variables represent either corridors or barriers, Circuitscape relies on resistance surfaces to represent the permeability of the landscape. However, defining the resistances to the movement of animals induced by those different environmental variables is challenging (eg. Janin, Léna, Deblois, et al. 2012; Trochet et al. 2019). Therefore, many studies rely on expert opinion to set their resistance values before using them in the software (eg. Shirk et al. 2010; Churko et al. 2020).

To compensate for the lack of empirical background, one strategy is to then carry out a sensitivity analysis by testing different models where the relationship between the

environmental variable and the resistance it causes varies from linear to sigmoidal or logarithmic for example (eg. Rayfield, Fortin, et al. 2010; Churko et al. 2020). While this is useful to understand the influence of this relationship on the connectivity of the landscape and to assess the robustness of the model, it does not inform on which model is closer to reality. Another weakness of this approach is that it does not allow to combine different environmental variables that might influence each other.

Another strategy, so far rarely chosen by scientists, is to use the expert opinion as a starting point to create resistance surfaces and then confront the output of Circuitscape to empirical data such as genetic distance or animal activity to identify the model that best fits them (Shirk et al. 2010; Finch et al. 2020). This can then be done for several environmental variables separately or combined. This strategy relies on the assumption that the measured data (genetic distance, animal activity, etc.) correlates with the connectivity of the landscape for the species of interest. However, the studies that explored this framework only validated the model without exploring much of the role of each environmental variable for the overall landscape resistance and resulting connectivity.

In both strategies, the number of models tested is limited by the computation time of Circuitscape. By transferring the environmental information to a regular grid network overlaying the study area, the computational time can be greatly reduced allowing for more testing. Such a grid network also offers the opportunity to model the connectivity of the landscape for multiple species and compare them with each other to generalize results found for individual species.

Because amphibians have a biphasic life-cycle and complex movement ecologies (Pittman et al. 2014), they have been heavily impacted by human transformation of the landscape (Cayuela et al. 2020). More than any other organism, they rely on this combination of blue and green infrastructures to thrive. Moreover, their low vagility compared to other organisms of their size and their population dynamics make them particularly sensible to landscape fragmentation (Catenazzi 2015). Altogether, this makes amphibians the perfect study species to assess the importance of various environmental variables for connectivity.

The main goal of this study was to model the connectivity of the landscape for amphibians and in the process identify its sensitivity to various resistance models for individual environmental variables known to drive the movement pattern of amphibians. The multi-species assessment relied on a network representation of the landscape to reduce computational time. The following research questions were answered:

1. What are the relationships between environmental variables and the resistance they cause for amphibian movement in human dominated landscapes? Can we identify and explain differences between species?

2. What is the relative importance of each of these variable as barriers or corridors for amphibian movement and how does this relative importance compare between species?

Firstly, I systematically explored a range of resistance models for individual and combined environmental variables important to amphibian movement. I then selected the best resistance model by identifying the resulting connectivity model that statistically best fitted empirical data. Secondly, I assessed the relative individual and combined importance of the variable's barrier or corridor effect by comparing the resistance they induce for amphibian movement. Thirdly, the relative importance of each environmental variable for amphibian landscape connectivity was assessed and compared between species. Finally, I compared my results with existing literature.

Chapter 2

Material and Methods

2.1 Modelling connectivity

Circuitscape (CS) is a software developed by Brad H. McRae et al. (2008) to model landscape connectivity by combining electrical circuit theory and random walk theory. It relies on the isolation by resistance model introduced by Brad H. McRae (2006). This model consistently outperformed until then traditionally used isolation by distance and least cost path models when predicting genetic differentiation (Brad H. McRae and Beier 2007).

The principle of this software is such: in a network of nodes and edges representing the landscape, a source of current is applied to a node A and a node B is connected to ground allowing the current to flow through the network. When each edge between two nodes represents the resistance of the landscape, the current will spread out in the network between node A and B following Ohm's law: $I = V/R$. It states that the amount of current I moving between two nodes is proportional to the voltage V and inversely proportional to the resistance R between the two nodes. In the electrical circuit that the network represents, the configuration of the resistances/edges in parallel or in series will also influence the distribution of the current in the network (Brad H. McRae et al. 2008).

Conversely, the random walk theory assumes that: an animal having only a proximal knowledge of the landscape, moving through a network representing that landscape from a node A to a node B, will make direction decision at each intersection based on the relative resistance of the different possibilities ahead of him. When repeating this trip form A to B numerous times with different animals, the probability of passage through each edge is proportional to its resistance (Doyle et al. 2000; Brad H. McRae et al. 2008).

Combining those two theories, the amount of current going through each node or edge is relative to the probability of a random walker going through that node/edge when moving from node A to node B (Chandra et al. 1996; Brad H. McRae et al. 2008). When

considering multiple node pairs, the current resulting from all the node pairs is summed for each node/edge of the network. The cumulative current measured at any location of the network is, therefore, a representation of the facilitating (corridor) or inhibiting (barrier) character of the landscape (Brad H. McRae et al. 2008).

2.2 Circuitscape set-up

I used CS in pairwise mode and a range of environmental variables as input for resistance models and fitted the results to abundance data of amphibian species to identify the best model of connectivity. The next three subchapters describe in more details the modelling choices driven by CS requirements.

2.2.1 Study area

Computation time has been optimized in CS but remains a limiting factor. Therefore, a case study area was selected in order to reduce the computation time for each resistance model tested. I limited the study to a ∼13 km circle radius located North-East of the city of Aarau in the canton of Aargau in the center of Switzerland (Figure 2.1). The circle shape was selected to minimize border effects in CS due to the low perimeter to area ratio of this geometry, the size was chosen empirically. The study area covers densely populated clusters mixed with agricultural fields in the valley bottoms. The North-West of the study area covers the foothills of the Jura mountains less densely populated. Three main rivers, the Aare, the Reuss and the Limmat cross the area before meeting at a confluence in the North-East. Two major highways (Highway 1 and 3) converge near the middle of the circle and a number of railway tracks of various importance also cross the area. To further reduce the border effect bias, the results used for calibration were limited to an inner circle of ∼8km radius later called calibration area, in pink in Figure 2.1. This buffer is superior to the distance Koen, Bowman, Sadowski, et al. (2014) suggested as minimal to avoid border effects in connectivity modelling.

2.2.2 Choice of network

Computation time was further reduced by the use of networks instead of rasters as input for CS. By simplifying the representation of the landscape, networks reduce the processing time in CS. Networks have been widely used in ecology to model connectivity at the landscape level (Rae et al. 2007; Rayfield, Fortin, et al. 2010; Godet et al. 2020). Whereas most studies create their networks based on the ecology of their species of interest with the node representing known populations or favorable patches of habitat and the edges the habitat matrix or corridors for example (eg. Decout et al. 2012), I opted for a

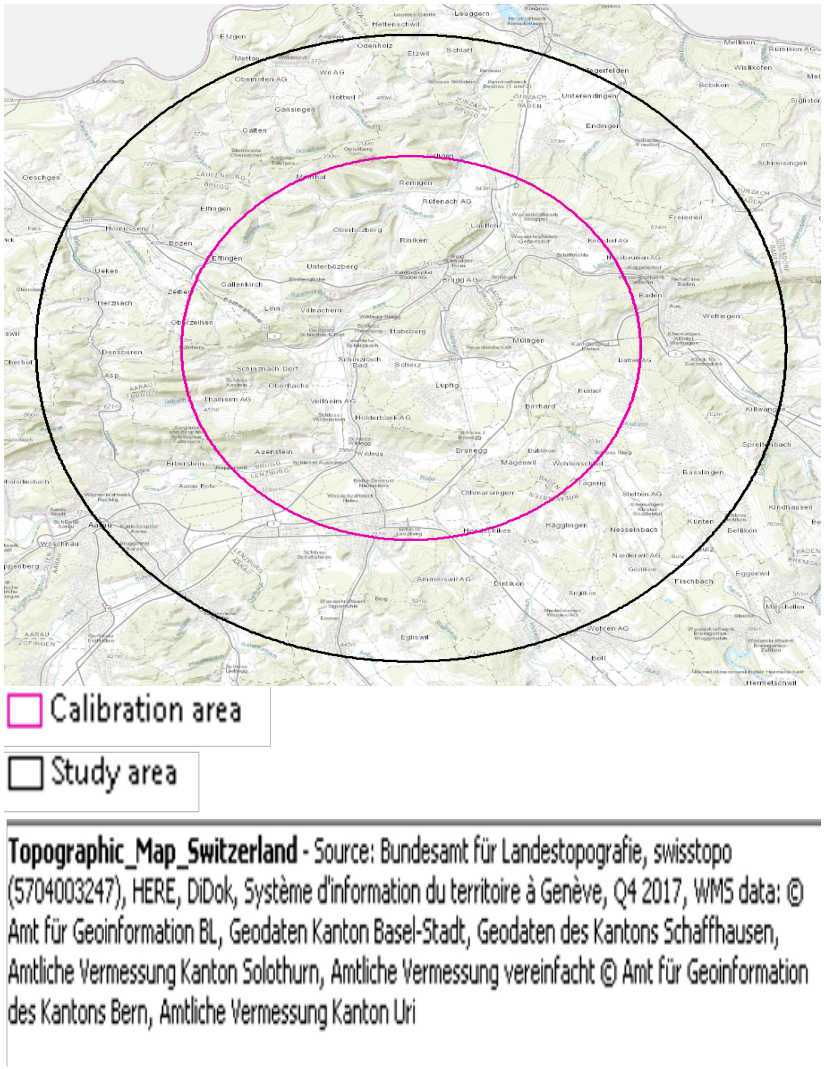

Figure 2.1: Study and calibration area

regular grid network covering the study area. This was done in order to have a relatively high current resolution while being able to run a high number of resistance models in CS in a lesser time. It also enabled me to use the same network for all species.

The network was based on a cover of hexagons over the study area where the centroids of each hexagon defined a node. All centroids were then connected to those of the neighbouring hexagons to create the edges of the network. Hexagons were chosen because they are the geometry closest to a circle allowing a regular tiling which results in a triangular planar grid where all nodes are connected to six edges of 519.62 m (Figure 2.2 (e)). The hexagons were clipped to the study area which caused the network to be slightly irregular on its outskirt. The whole network was composed of 6805 edges and 2337 nodes, the calibration area contained 835 nodes. All the species and environmental data used in this study then had to be transposed to this network. The different data sets and how they were transposed are described in the chapters 2.3 and 2.4.

2.2.3 Choice of focal nodes

The focal nodes are the nodes of the network where the current will be applied in CS. To force the current to move through the whole study area I selected node pairs in a circle around the calibration area similarly to what Koen, Bowman, Sadowski, et al. (2014) experimented (Figure 2.2 (e)). They were set to be approximately at a 4° angle from each other and at around 11000 m from the center of the study area. It was estimated that this distance was enough to minimize any current bias from the focal nodes in the calibration area (Koen, Bowman, Sadowski, et al. 2014). In the runs of CS each node was connected only to the node directly on the opposite side of the circle in a pairwise manner. In total, each run of CS compiled the current of 45 pairs of nodes. This is more than what Koen, Bowman, Sadowski, et al. (2014) used for their landscape composed of 10 000 pixels (equivalent to the nodes of the network). Following this study's conclusions, it was estimated that no sensitivity analysis on the number of nodes was needed because they could not observe a penalty in including to many nodes.

This choice of focal nodes results in modelling the structural connectivity of the landscape because those nodes do not represent the actual occurrences of the species. The current at a given node/edge, therefore, only reflects its importance for the connectivity of the whole network solely based on landscape characteristic. Taking into account the increased importance of that node/edge for the species because of its location relative to the surrounding known populations/occurrences would have resulted in modelling the structural connectivity of the landscape for each species. An attempt at achieving this using known breeding sites of the species as focal nodes was made but later discarded due to other shortcomings (for more on this see Appendix B).

2.3 Fitting data

To assess the quality of the connectivity models produced by CS, they were fitted to empirical data collected in the study area. The next two chapter describe these data and how they were transformed to fit the network approach.

2.3.1 Choice of study species

Amphibians were chosen as study organism because their rich movement ecologies and population dynamics make them sensible to landscape fragmentation (Catenazzi 2015; Cayuela et al. 2020). Their distribution should therefore be closely related to connectivity (Decout et al. 2012). Switzerland counts 19 amphibian species, five were selected for this study. Including diverse species to reflect the variety of ecological niches and movement ecologies of amphibians in the Swiss lowlands should allow a good overview of landscape

connectivity for amphibians (Beier et al. 2008). In addition, I included both urodeles and anurans as well as mobile and less mobile species. I also tried to include well distributed alongside rarer species.

1. *Bufo bufo*: a relatively mobile toad species with strong migration pattern (Sztatecsny et al. 2005). It is found throughout Switzerland and can be considered a generalist. It roams the breeding sites only for a short time period and does not rely much on them for the rest of the year (KARCH 2020).

2. *Epidalea calamita*: a toad species that mostly relies on temporary water bodies in fields or gravel pits. This pioneer species is endangered by the drainage of the fields and the canalisation of rivers that prevent the formation of the temporary ponds it depends on (KARCH 2020).

3. *Hyla arborea*: a threatened anuran (Angelone et al. 2009). Adults spend most of their life up in the vegetation and return to ponds for breeding but do not show site fidelity like most other amphibians (KARCH 2020).

4. *Ichthyosaura alpestris*: a very wide spread generalist pioneer and the most mobile Swiss urodele. It quickly colonizes newly formed ponds (KARCH 2020).

5. *Rana temporaria*: the most widely spread amphibian species in Switzerland. This anuran can colonize water bodies of all sizes and is, therefore, considered a generalist even though it relies more on forested environments (Decout et al. 2012). Similarly to *B. bufo* it does not rely much on water bodies outside of the breeding season (KARCH 2020).

2.3.2 Amphibian data and interpolation to the network

The amphibian data came from a long term citizen science monitoring program conducted for the Canton of Aargau Switzerland (Bühler 2019). The number of monitored sites increased from around 600 in 1999 to 1500 in 2020. 300 sites are sampled more or less randomly each year and are visited three times for a duration determined by their size. From this data set, the cumulative number of adults, juveniles and calls reported for each visit was used as proxy for the long-term population size. This number was averaged for each site across visits and over the whole monitoring period using the *aggregate* function from the "stats" R package (step 1.1 in the conceptual model in Figure 2.4) (R Core Team 2019). This average will be referred to as "site average" in the following.

Because population demographics are not necessarily well related to the patterns of distribution (Cushman 2006; Martensen et al. 2012), a first attempt at using the site average to fit the connectivity models yielded low correlation. It was therefore decided to interpolate the data based on a simplified inverse distance weighting (IDW) in order

to have a representation of the distribution of the species combined with abundance information.

For each node of the network described in chapter 2.2.2 a 500 m radius circular buffer was considered. The distance of 500m was chosen because it was considered to reflect the movement abilities of all five study species (Miaud et al. 2000; Angelone et al. 2009; Kovar et al. 2009; Le Lay et al. 2015). The sum of the site average divided by the distance from the site to the node was computed for all the survey locations found in this buffer. This sum was then attributed to the node considered (step 1.2 in the conceptual model in Figure 2.4). The distance was computed by the *st_ distance* function from the "sf" R package and the sum was computed by the *aggregate* function from the "stats" R package (Pebesma 2018; R Core Team 2019). Nodes for which no survey location in the 500 meters buffer existed were given the value of 0 and are later called absences. The nodes to which a value could be attributed are called presences.

2.4 Environmental variables important for amphibian movement

Four environmental variables were selected in order to capture most of the resistance amphibians encounter when roaming the landscape (Figure 2.2 (a), (b), (c) and (d)). The next subchapters will present the reason for choosing these variables, how they were computed and represented in the network.

2.4.1 Shortest distance to water

The amphibian life-cycle is closely related to water as most of them rely on an aquatic environment during one of their life-stage. Due to their low vagility, it is expected that the distance to the nearest water body limits their movement and thus induces a resistance to movement. The shortest distance to water should, therefore, be positively correlated with resistance (Westgate et al. 2012).

This information was computed by first retrieving lotic, lentic and reed belt (Gewaesser stehendes/fliessendes, schilfguertel) polygons from the "Land cover" (Bodenbedeckung) layer of the cadastral map of the Canton Aargau (Vermessungsamt des Kantons Aargau 2020). These polygons were first rasterized at a 10 m resolution using the *rasterize* function from "raster" R package (Hijmans 2020). To optimize the detection of small water bodies (conservative rasterization), the polygons were rasterized once as polygons and a second time after being projected as lines using the *st_ cast* function form the "sf" R package (Pebesma 2018). These six rasters were then combined and the distance to the nearest water cell was then computed for the whole canton using the *distance* function

from the ″raster" R package (Hijmans 2020). Finally, the mean value of the raster cells in a 10 m buffer around each edge was used to transpose the data to the network using the *extract* function form the R package "raster" (step 2.1 in the conceptual model in Figure 2.4).

2.4.2 Slope

Slope also affects amphibian movement and is one of the most researched factor of gene exchange according to Cayuela et al. (2020). But it seems that not all species are impacted in the same way (Sztatecsny et al. 2005). Nonetheless, it is expected that the slope is positively correlated with resistance for all species (Lowe, Likens, et al. 2006; Westgate et al. 2012).

It was derived from the Swiss Topographical Landscape model (swissTLM 3D 2015) at 2 m resolution (elevation uncertainty ± 0.5m) using the *slope* function in ArcGIS 9.3 software (ESRI 2008) and subsequently aggregated to a median value using the *aggregate* function implemented in the "raster" R package (Hijmans 2020). Similarly to the shortest distance to water the mean value of the raster cells in a 10 m buffer around each edge was used to transpose the slope to the network using the *extract* function form the "raster" R package (step 2.1 in the conceptual model in Figure 2.4)(Hijmans 2020).

2.4.3 Traffic

Traffic has been used by many studies as proxy for the barrier effect of roads for amphibian movement (eg. Joly et al. 2003). Again, the exact role of this environmental variable for landscape connectivity seems to be species specific but it is expected that for all of them the resistance should be positively correlated with traffic (Mazerolle et al. 2005).

The data from the "National Traffic Model" (Nationales Personenverkehrsmodells) was used under the form of an ESRI Shapefile where lines representing the roads contained information on traffic intensity (Justen et al. 2017). The daily number of vehicles passing at the intersections with the network were summed for each edge and used as proxy for resistance (step 2.1 in the conceptual model in Figure 2.4). This was achieved using the *st_intersection* and *aggregate* functions from the "sf" and "stats" R packages respectively (Pebesma 2018; R Core Team 2019).

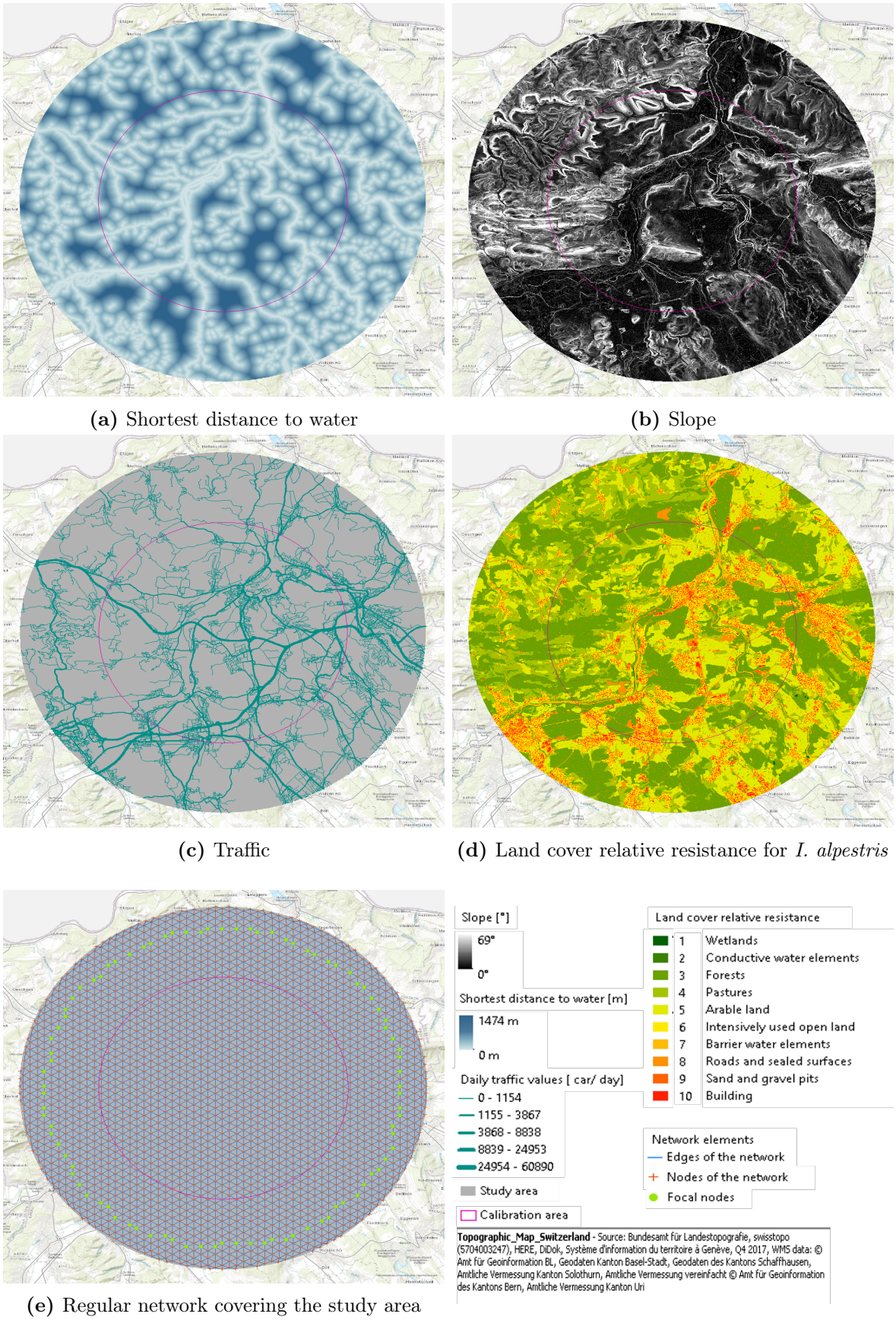

(a) Shortest distance to water

(b) Slope

(c) Traffic

(d) Land cover relative resistance for *I. alpestris*

(e) Regular network covering the study area

Figure 2.2: Environmental variables and network over the study area

2.4.4 Land cover

Amphibian species rely on various habitat to thrive, while some prefer forests like *R. temporaria* others seem to be better adapted for agricultural land as *E. calamita* (Frei et al. 2016; KARCH 2020). Each land cover, therefore, causes a defined resistance to the movement of amphibians and this resistance is species specific. The relative resistance of each land-cover for the study species is what I tried to model here. The first step was therefore to create land-cover classes relevant from an amphibian movement point of view. Once again the "land cover" layer from cadastral map of the canton of Aargau was used and reclassified (Vermessungsamt des Kantons Aargau 2020). Additionally, some features from the layer "single objects" (Einzelobjekten) where also considered if they were relevant for amphibian movement. The reclassification choices are explained in Appendix A.1 and the end results can be seen in Table A.1 of this appendix. The classes were chosen to fit those of Churko et al. (2020) but some adjustment were necessary. Furthermore, recombining the existing class was sometimes insufficient, the methods used to improve the classes are described in the next two paragraphs.

The cadastral map did not make any difference between arable land and pastures but both do not have the same impact on amphibian movement (Janin, Léna, Ray, et al. 2009; Cayuela et al. 2020). To further classify the agricultural land, I used a data set from Pazúr et al. (2021b). The data set is a raster of 10 m resolution produced from the Sentinel-2 bands and additional indices based on the vegetation phenology (mostly naturalised difference vegetation index/NDVI-based) (Pazúr et al. 2021a). Each cell of the raster is given either the value 1 for arable land, 2 for grassland or no value for other land covers. The mean value of the cells inside the agricultural polygons from the cadastral map was computed using the *extract* function from the "raster" R package (Hijmans 2020). All polygons with a mean higher than 1.5 were classed as pastures, whereas polygons with a lower mean were classed as arable land. Because the raster and the polygons were not a perfect match, some agricultural polygons ended with no value. After verification most of these polygons were either small roadside fields, greenhouses, gravel pits, etc. It was therefore decided to class those polygons in the "intensively used open-land" class. Even though this choice might have lead to minor misclassification, it is expected that due to further data transformation it should not have had too much impact on the end results.

Additionally, the cadastral map classification of the water element did not allow to differentiate between big and small lakes/rivers. It also mostly regroups the water bodies and their banks which represent valuable habitat and possible corridors for amphibians, whereas open water might be a barrier to them (Angelone et al. 2009; Covarrubias et al. 2020). Therefore, I further classified the water elements by applying a negative 5 m buffer to them. All parts of the polygons within this buffer were deemed rather favorable and classed as conductive water elements, whereas the elements further away from the side of

the polygons were classed as water barriers.

Finally, the different classes obtained were ranked from the least resistant to the most resistant and given values accordingly from 1 to 10 later called relative resistances. This relative resistance of the classes is expected to be species specific. For example, arable land may not cause much resistance for the movement of *E. calamita* relatively to forests but the opposite is true for *I. alpestris* for which forest causes less disturbance than arable land (Emaresi et al. 2011; Frei et al. 2016). Therefore, the ranking was done for each species separately. The resulting relative resistances obtained for each species can be seen in Table A.2 of appendix A.1 as well as the literature background justifying the choices made.

Because this relative resistance of the land-cover is a discrete value attributed to polygons, the representation of the information in a network is more complex than for the other variables. It has been done in a slightly different way explained at the end of chapter 2.5.1.

2.5 Modelling landscape resistance

Although the four environmental variables presented above induce some resistance for amphibian movement, they do not represent resistance directly. Shirk et al. (2010) introduced a framework to model and calibrate landscape resistance induced by environmental variables in order to improve the quality of genetic isolation models. Their work showed the importance of the calibration to accurately represent the relationship between the variable of their model on the one hand and the resistance they induced for gene exchange on the other hand. Finch et al. (2020) could make similar conclusion when applying the framework to commuting bats to model landscape connectivity. The next chapters detail how this framework was applied in the present case study.

2.5.1 Resistance models

Similarly to what Shirk et al. (2010) and Finch et al. (2020) tested, I wanted to investigate the relationship between the variables of my connectivity model and the resistance they induce for amphibian movement. To uncover that, I used the framework from Shirk et al. (2010) and computed different resistances models based on the value of the variable given to the edges in the previous step using the following equation (step 2.2 in the conceptual model in Figure 2.4):

$$R = (Var/Var_{max})^x * RMax + 1$$

Where Var is the value of the variable in the given edge of the network. Var_{max} is the maximum value of the variable encountered in the network. x is a parameter that was first allowed to vary between 0.1 and 20 but later extended from 0 to 70. It dictated the slope along which the resistance increased when the variable increased or in other words the shape of the relationship between the variable and the resistance. For a given edge, the resistance decreased when the parameter x increased. In contrast, $RMax$ defined the resistance of the edge with the highest value of the variable in the network or the range of resistance values of the model. At first it was allowed to vary from 5 to $5 * 10^5$ but was later extended to 1 to $1 * 10^{13}$. Indirectly, this also influenced the slope of the different resistance models. For a given edge, the resistance increased when $RMax$ increased. Each combination of x and $RMax$, later called parameter set, created a unique resistance model. This relationship between the variables and the resistance they cause to the movement of amphibians can be seen in Figure 2.3.

The resistance models for the land cover were computed in a slightly different way than the other environmental variables. Each land cover class described in chapter 2.4.4 is expected to cause given resistance to amphibian movement such that they can be ranked from the least resistant to the most resistant. The influence of this relative resistance on the connectivity is what I want to explore. It would not impact connectivity directly if the resistance model was applied after the information of the land cover polygons has been aggregated to the edges of the network. Therefore, the resistance models were computed with the same equation presented above at the level of the land cover polygons where Var is the relative resistance of the class of the polygon and Var_{max} equals 10, the relative resistance of the highest class in the ranking. This means each polygon of land cover was given a value of resistance for each resistance model (step 2.3 in the conceptual model in Figure 2.4). For the transposition to the network, only the polygons within a 10 m buffer around each edges of the network were considered, similarly to the other variables. Before the transposition, this resistance was multiplied by the percentage of the buffered edges that the polygon covered (step 2.4 in the conceptual model in Figure 2.4). Finally, the values obtained for the polygons within each buffered edge were summed and used as resistance in CS (step 2.5 in the conceptual model in Figure 2.4). This sum was taken using the *aggregate* function from the "stats" R package (R Core Team 2019). Through this transformation the effect of the model was damped. Therefore, it is expected that the correlation between the connectivity models resulting from the land cover and the interpolated abundance will be more stable between resistance models than for other variables.

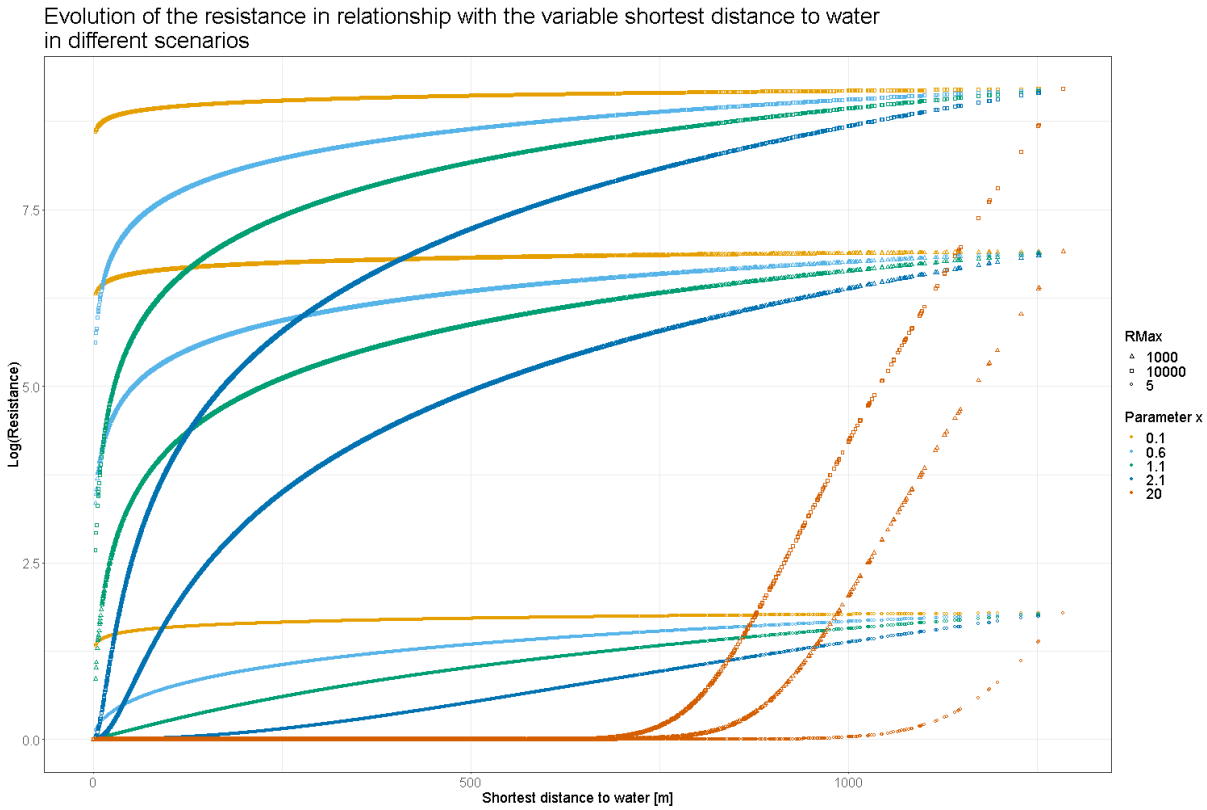

Figure 2.3: Evolution of the resistance in relationship with the shortest distance to water in different models. Each line represents a model/parameter set and each point of a line is one edge of the network. The color of the lines indicates the value of the parameter x for that model, the shape of the points illustrate the value of $RMax$. Different lines of the same colors show the impact of varying $RMax$. All the lines converging in single points at the right of the graph show the effect of varying x. The value to which they converge corresponds to their respective $RMax$. Note the logarithmic scale of the y-axis.

2.5.2 Univariate calibration

The models of landscape resistance were computed for the four environmental variables: shortest distance to water, slope, traffic and land cover. Additionally, one network where all edges had the same resistance similar to the isolation by distance scenario from Shirk et al. (2010) was created (later called no variable scenario). It was run in CS to investigate the effect of the topology of the network and the focal nodes set on the current and the correlation with the interpolated abundance data (for more on this sensitivity analysis refer to the appendix B). Similarly to what Shirk et al. (2010) and Finch et al. (2020) experimented, each weighted network obtained by computing models of landscape resistance was used separately as resistance layer in CS with the focal nodes described in chapter 2.2.3 (step 3.1 in the conceptual model in Figure 2.4). In the output connectivity

model, the current in each node/edge results from their own resistance and the resistance of the surrounding edges as well as their position in the network following the principle presented in chapter 2.1.

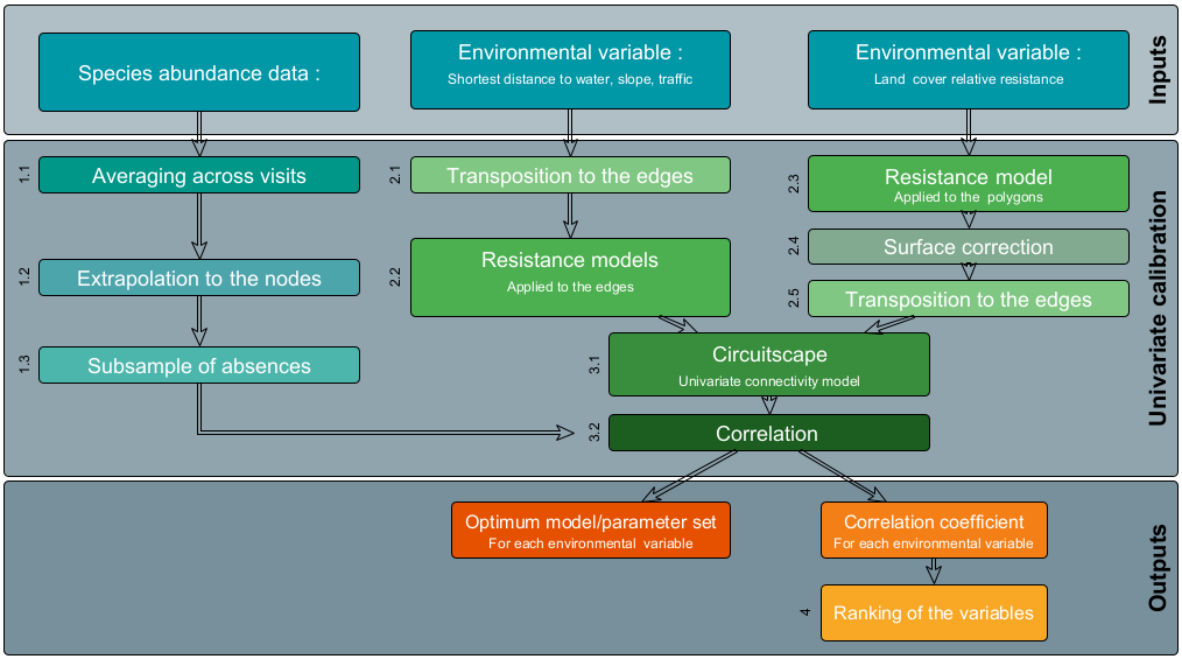

Figure 2.4: Conceptual model of the univariate calibration

To identify each variable's resistance model that best represented landscape connectivity for the species at hand, I tested for the performance of the connectivity model resulting from each resistance model. I first subsampled a number of absences equal to 1.5 times the number of presences (step 1.3 in the conceptual model in Figure 2.4). Chapter B.2 in Appendix B gives more information on the choice of this number. Then, the Spearman's rho between the current of the connectivity model at the nodes and this subsample of the interpolated abundance data was computed (step 3.2 in the conceptual model in Figure 2.4). The model with the best correlation should be the most accurate representation of landscape connectivity allowed by the variable. This is based on the hypothesis that the combination of distribution and abundance represented by the interpolated abundance data is a good approximation of the probability of observing an individual at any given location. This probability should in turn be higher at locations (here the nodes of the network) which are better connected and thus have higher current (Rosenberg et al. 1997; Uezu et al. 2005; Koen, Bowman, Sadowski, et al. 2014).

Because the resistance model has two parameters (parameter x and $RMax$) the solution space can be represented in 3D graphs as shown in Figure 2.5. From these graphs, the parameter sets with the highest correlation were identified for the four variables separately. Finally, the variables were ranked based on the correlation they yielded (step 4 in the conceptual model in Figure 2.4).

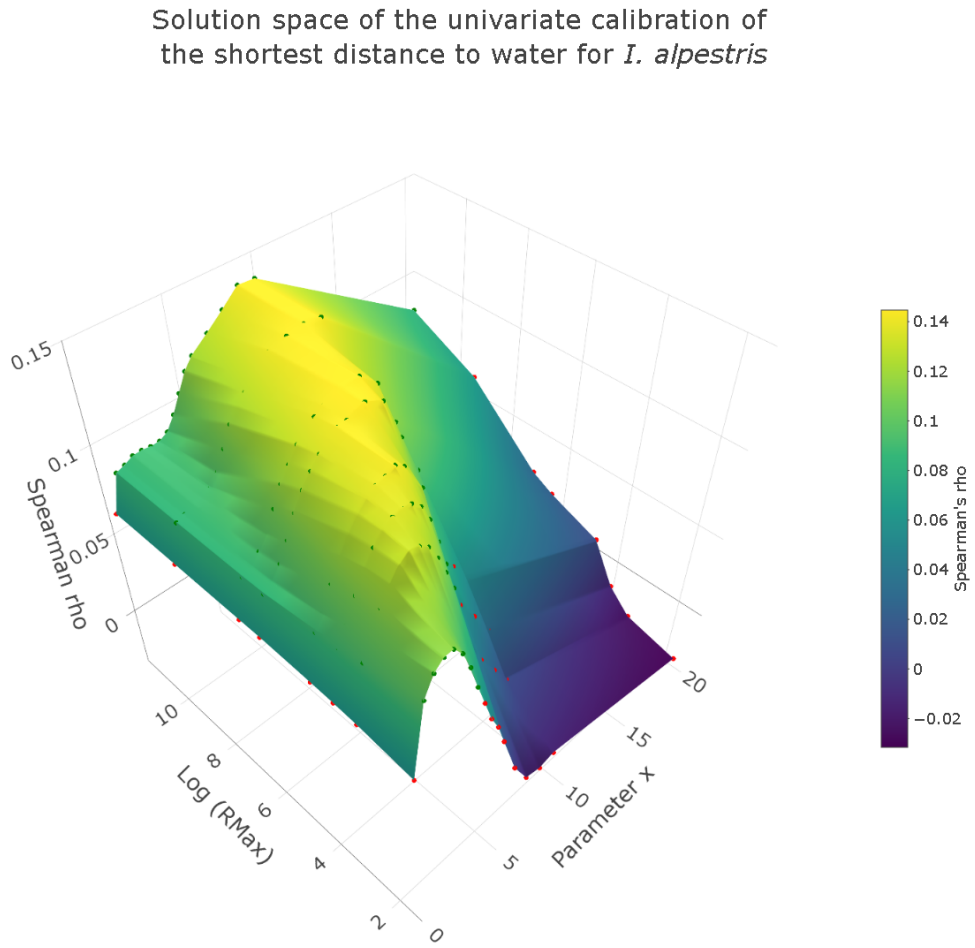

Figure 2.5: Solution space of univariate calibration of the shortest distance to water for *I. alpestris*. The surface shows the correlation between the connectivity models and the interpolated abundance data. The parameter x of the resistance model is represented on the x-axis and the logarithm of $RMax$ on the y-axis. The correlation is given on the z-axis. Each point represents a parameter set/model, the color of the point indicates whether the correlation is significant or not (Green = significant, red = insignificant)

2.5.3 Multivariate calibration

Connectivity at the landscape level does not result from single variable but is rather a combination of interacting components (Zeller et al. 2012). To account for these possible interactions, the variable's models were calibrated together in a second step in the same process experimented by Shirk et al. (2010) and Finch et al. (2020). Only the variables that yielded significant correlation in the univariate calibration were kept in this multivariate model with the threshold set at the p-value of 0.05. Because more than 136 resistance models per variable were computed in the univariate calibration, it was computationally impossible to test all the combinations and run them in CS fro each species. Therefore, new resistance models were computed for a single variable at a time (the dynamic variable) in just the same way as the univariate calibration. The variable that obtained the highest correlation in the univariate calibration round (ranked first at step 4 in Figure 2.4) was used as first dynamic variable .

The resistance resulting from the optimum parameter set of the other variables (static variables) was then added to those new models of the dynamic variable resulting in the multivariate resistance models (step 5.1 in the conceptual model in Figure 2.6). This combined resistance network was then used in CS to compute a multivariate connectivity model (step 5.2 in the conceptual model in Figure 2.6). Finally, the Spearman's rho was computed again for the correlation between the current of the connectivity model and the interpolated abundance data (step 5.3 in the conceptual model in Figure 2.6). This allowed to identify in the two dimension solution space the optimum parameter set for the dynamic variable when interacting with the other variables.

In a next round of calibration, the variable with the second best correlation in the univariate calibration (ranked second) was set as the dynamic variable. The optimum parameter set just identified was used as static variable along with the remaining variables and added to the resistance of the current dynamic variable models (Decision 6.1 in the conceptual model in Figure 2.6). These were again run in CS to identify the optimum parameter set of this second dynamic variable using Spearman's rho. These steps were repeated for all variables down to the one with the lowest correlation (ranked last) (Decision 6.3 in the conceptual model in Figure 2.6). However, if the optimum parameter set of one of the variable ranked lower than first differed from that previously identified for that variable (univariate or multivariate calibration), the process started over again with the variable ranked first as dynamic variable and these new optimum parameter set as static variables (Decision 6.2 in the conceptual model in Figure 2.6).

In this process, I was looking for a combination of parameter sets (one per variable) that maximises the correlation of the connectivity model with the interpolated abundance. Because the resistance of each variable is modified by two parameters (Parameter x and $RMax$), the solution space of the multivariate calibration was composed of six to eight dimensions depending on how many variables were selected for the multivariate calibration. However, by fixing the values of some of the variables at each round (static variables), I was able to explore those six/eight dimensions two at a time to find a global optimum similarly to the univariate calibration.

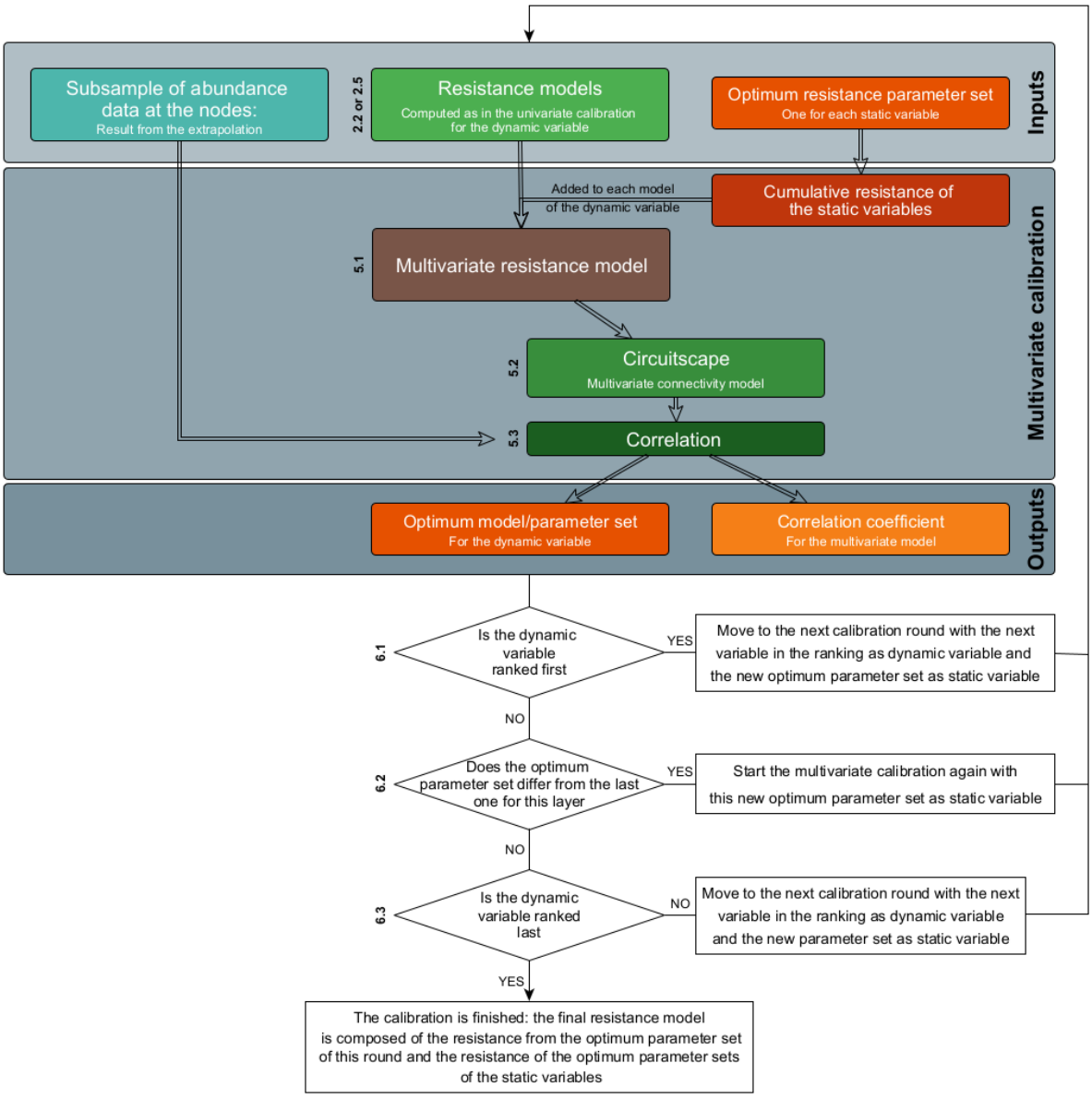

Figure 2.6: Conceptual model of the multivariate calibration

Chapter 3

Results

3.1 Abundance interpolation

The interpolation of the abundance data to the nodes of the network had an impact on the distribution of the values (Table 3.1). Taking the site average decreased the range of value and thus the standard deviation. The mean value also decreased for all species except *R. temporaria* for which it was not impacted. The median and the skewness had inversely proportional reactions but the direction of the change was not the same for all species. Overall, all the indicators stayed within the same order of magnitude.

Table 3.1: Overview of the effect of the interpolation of the abundance data on the distribution of the values

Species	State of the data	Presence/Absence	Minimum	Maximum	Mean	Median	Standard Deviation	Skewness
B. bufo	Raw	Both	0	100	1.69	0	7.27	9.57
	Site average	Both	0	16.17	1.32	0.96	2.11	4.17
	IDW	Both	0	8.24	0.25	0	0.82	5.62
	IDW	Presence	0.03	8.24	0.98	0.49	1.38	2.90
E. calamita	Raw	Both	0	30	4.21	2	5.76	1.94
	Site average	Both	0	15	2.79	2	3.20	2.33
	IDW	Both	0	11.21	0.11	0	0.67	11.35
	IDW	Presence	0.11	11.21	1.48	0.85	2.05	3.26
H. arborea	Raw	Both	0	183	28.82	4	42.83	1.55
	Site average	Both	0.50	54.69	4.65	1	12.21	3.91
	IDW	Both	0	55.17	0.16	0	2.17	21.33
	IDW	Presence	0.20	55.17	3.59	0.56	9.80	4.30
I. alpestris	Raw	Both	0	250	8.98	3	18.56	6.3
	Site average	Both	0	63	6.70	4.47	8.05	3.44
	IDW	Both	0	51.91	1.57	0	4.32	6.36
	IDW	Presence	0.11	51.91	4.36	2.29	6.32	4.30
R. temporaria	Raw	Both	0	51	1.50	0	4.89	6.18
	Site average	Both	0	27.50	1.50	0.50	3.54	4.99
	IDW	Both	0	45.05	0.38	0	2.15	14.64
	IDW	Presence	0.03	45.05	1.48	0.42	4.04	7.75

After the interpolation, the maximum value decreased for all the species except *R. temporaria*. On the other hand, the minimum number of observed individual increased except for *H. arborea*. When taking only the presences into consideration, the mean, the median and the standard deviation did not vary much after the interpolation but decreased slightly for all the species. The skewness increased for all species except for *B. bufo* but stayed in the same order of magnitude as well.

Looking at the interpolated data, *I. alpestris* was the most wide spread species with 300 nodes of the network out of 835 in the calibration area having presences (Table 3.2). It was also one of the most abundant with up to 51.91 observations and a mean of 4.36 observations per node where it was present. *B. bufo* and *R. temporaria* are also well distributed across the calibration area. However, the second showed higher concentration of individuals than the first as well as a higher mean per node even though it was more skewed. *B. bufo* was the most evenly distributed species across the nodes with a skewness of 2.90 and a standard deviation of 1.38. *E. calamita* came fourth in terms of distribution with 61 nodes to which presences could be attributed. Finally, *H. arborea* was the last species in terms of distribution across the nodes, being present at only 37 of them but it showed the highest concentration of individuals at a single node with a maximum of 55.19 just above *I. alpestris*. It also had the highest minimum with at least 0.20 individuals if observed at all.

Table 3.2: Number of nodes of the calibration area for which abundance data could be interpolated (presences) and consequent number of nodes without abundance data sampled for the calibration (absences)

Species	Presences	Absences
B. bufo	216	324
E. calamita	61	92
H. arborea	37	56
I. alpestris	300	450
R. temporaria	216	324

3.2 Network representation of the environmental variables

Similarly to the interpolation of the abundance data, transposing the environmental variables to the network following the method described in chapter 2.4 and 2.5.1 for the land cover had an effect on the distribution of the data (Table 3.3). For the variables shortest distance to water and slope, all indicators stayed in the same order of magnitude indicating a rather small effect. For the traffic variable: the range, the mean and the standard deviation increased from more than an order of magnitude, whereas the median

stayed the same. Even though the skewness decreased for that variable, it was still highly skewed towards lower values because many edges did not intersect any roads or only roads for which the daily traffic was deemed to be null. The values for the land cover in Table 3.3 are the direct transposition of the relative resistance to the network without applying the resistance model to allow comparison with the other variables (skipping step 2.3 in the conceptual model in Figure 2.4). This variable was more strongly impacted by the transposition than the other variables. While the range and the standard deviation stayed relatively stable, the mean and the median decreased significantly with the transposition. The median was halved for the relative resistance of most species. Furthermore, the skewness shifted from negative to positive for all species.

Table 3.3: Overview of the effect of the transposition of the environmental variables into the network on the distribution of the values. The values for the land cover are presented for the relative resistance of the land cover classes of the five species. They were computed for the direct transposition of the relative resistance to the network without applying the resistance model (skipping step 2.3 in the conceptual model in Figure 2.4) for comparison purpose.

Variables	State of the variable	Min	Max	Mean	Median	Standard deviation	Skewness
Shortest distance to water [m]	Original	0	1446	289	240	230	1.10
	Network	0	1284	288	232	214	1.25
Slope [°]	Original	0	68.54	10.03	7.76	8.56	1.18
	Network	0	42.45	10.06	9.18	6.12	0.80
Traffic [vehicles/day]	Original	0	65270	975	0	3049	9.97
	Network	0	162767	4490	0	15167	6.16
Land cover [-] *B. bufo*	Original	1	10	8.7	10	2.1	-1.59
	Network	2.00	10.23	5.16	4.94	1.42	0.71
Land cover [-] *E. calamita*	Original	0	10	8.78	10	2.06	-1.94
	Network	0.71	10.29	4.75	4.82	1.99	0.28
Land cover [-] *H. arborea*	Original	0	10	8.49	10	2.26	-1.09
	Network	1.85	12.31	5.77	5.83	1.21	0.11
Land cover [-] *I. alpestris*	Original	0	10	8.70	10	2.10	-1.59
	Network	2.00	10.23	5.14	4.93	1.39	0.70
Land cover [-] *R. temporaria*	Original	0	10	8.62	10	2.39	-1.90
	Network	0.75	10.23	4.34	4.47	2.11	0.15

3.3 Univariate calibration

Table 3.4 summarizes the optimum parameter sets obtained for the resistance model in the univariate calibration round and the consequent Spearman's rho yielded by the connectivity models.

The current resulting from the shortest distance to water yielded the best correlation with the abundance data overall. However, the correlation difference between the shortest distance to water and the slope for *H. arborea* and *R. temporaria* was only of around 0.01 and 0.005 respectively. For this variable, the parameter x varied between 5.6 and 9.6,

except for *E. calamita* for which it reached the maximum value possible in the univariate calibration. The $RMax$ was set to the maximum value allowed for three out of five species for this variable.

The current resulting from the resistance of the slope and the traffic were often evenly correlated with the abundance data even though the slope was often on top. The correlation difference was bigger, however, for *H. arborea* for the reason mentioned above. The parameter x of the slope was rather stable between species varying only between 5.6 and 6.6 except for *I. alpestris* for which it was set to 2.6. The $RMax$ for this variable was also rather stable, often reaching the maximum value allowed in the univariate calibration.

Traffic was the variable for which the parameter x was the most undecided. For three of the species, it took the minimum value allowed of 0.1 and for the other two the maximum value allowed of 20. The $RMax$ for this variable, however, was similar to that of the slope for all species. It is to be noted that the correlation for the traffic was barely significant for *H. arborea*.

The land cover was the variable for which the correlation was the lowest for all the species. In fact, it was only significant for *I. alpestris*. Comparatively to the other variables it often took values of parameter x and $RMax$ leading to much lower resistance than the other variables. For *E. calamita*, $RMax$ had little impact on the correlation with all the values between 500 and $1 * 10^5$ yielding the same correlation when parameter x was set to 0.6.

Table 3.4: Summary of the results of the univariate calibration

Species	Variable	Parameter x	$RMax$	Spearman's rho	S statisitc	P value
B. bufo	Shortest distance to water	9.6	$1 * 10^5$	0.1478	22364494.27	0.0006
	Slope	5.6	$1 * 10^5$	0.1196	23105538.41	0.0054
	Traffic	20	$1 * 10^4$	0.1067	23444058.82	0.0131
	Land cover	20	5	0.0048	26116833.98	0.9106
E. calamita	Shortest distance to water	20	$1 * 10^5$	0.2571	443461	0.0013
	Slope	6.6	$1 * 10^4$	0.1776	490866.31	0.0280
	Traffic	20	$1 * 10^5$	0.1716	494447.4	0.0339
	Land cover	0.6	$500 : 1 * 10^5$	0.1471	509115.38	0.0697
H. arborea	Shortest distance to water	5.6	$1 * 10^5$	0.3228	90036.54	0.0013
	Slope	6.6	$1 * 10^5$	0.3091	92613.04	0.0026
	Traffic	0.1	$1 * 10^5$	0.2052	106539.48	0.0485
	Land cover	0.1	5	0.0224	131037.71	0.8310
I. alpestris	Shortest distance to water	6.6	500	0.1449	60127220.68	<0.0001
	Slope	2.6	$1 * 10^5$	0.0931	63763592.2	0.0107
	Traffic	0.1	$1 * 10^5$	0.1079	62723879.8	0.0031
	Land cover	0.6	5	0.0744	65078551.38	0.0416
R. temporaria	Shortest distance to water	6.6	500	0.1391	22594591.56	0.0012
	Slope	5.6	$1 * 10^5$	0.1347	22709944.57	0.0017
	Traffic	20	$1 * 10^4$	0.1033	23533175.11	0.0163
	Land cover	0.6	5	0.0663	24503663.76	0.1238

Overall, the species widely distributed (*I. alpestris*, *B. bufo* and *R. temporaria*) yielded lower correlations than the ones with fewer presences (*E. calamita* and *H. arborea*). No effect of the distribution of the abundance between the presence nodes could be observed on the strength of the correlation.

3.4 Multivariate calibration

3.4.1 The process

Between the rounds of calibration, the values of the parameter x varied between 0 and 70, whereas the $RMax$ could vary from several orders of magnitude and was rather reacting on a logarithmic scale. The Spearman's rho also fluctuated for the same models between rounds because of the sampling of different sets of absences. This variation was higher for rarer species because the absences sets could differ more from one round to another. This rendered the identification of the optimum parameter sets more difficult. To ease the process, I often computed the correlation between the current and the abundance data with a few sets of absences for the same multivariate resistance models to identify the most stable optimum. The number of model combinations tested varied between 700 and 1600 per species (Table 3.5).

In the solution space, the optimum were often located on ridges going from low parameter x and low $RMax$ to high parameter x and high $RMax$. Figure 2.5 and Figure3.1 (a) illustrate that well. The angle between the ridge and the x-axis as well as the sharpness of the ridge changed between the variables and the species. Sometimes, the correlation plateaued in front of the ridge leading to less blatant optimums as shown in Figure 3.1 (b). Finally, in other cases, the optimum parameter set formed an obvious peak. In such cases the optimum did not move much when the static variables changed. Such a peak can be seen in Figure 3.1 (c).

Table 3.5: Overview of the number of calibration round per variable and the number of models tested per species. The number of round of calibration is the number of time each variable has been set as dynamic variable excluding the univariate calibration round. The variation in the number of combination tested between the species comes from the number of values of parameter x and $RMax$ tested at each round.

Species	Number of round of calibration				Total number of model combination tested
	Shortest distance to water	Slope	Traffic	Land Cover	
B. bufo	9	9	3	-	1200
E. calamita	10	10	3	-	1600
H. arborea	4	4	1	-	700
I. alpestris	6	2	6	2	900
R. temporaria	6	6	3	-	1400

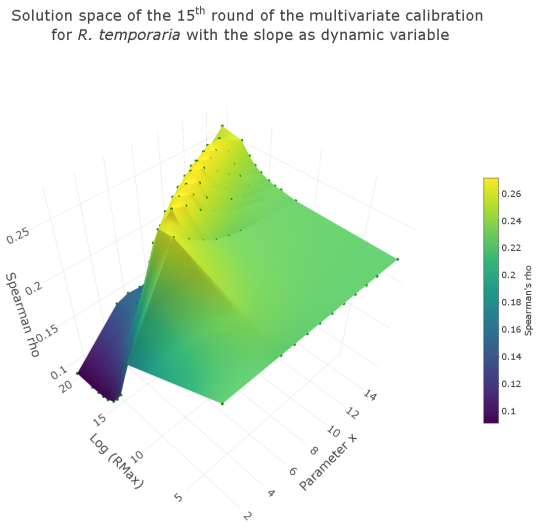

(a) Solution space of the 15^{th} round of the multivariate calibration for *R. temporaria* with the slope as dynamic variable

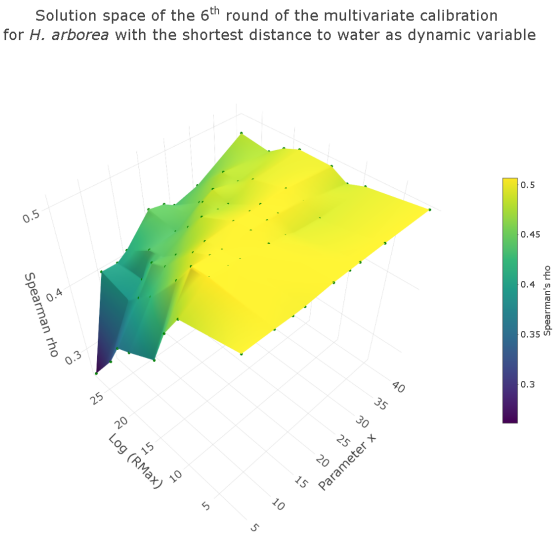

(b) Solution space of the 6^{th} round of the multivariate calibration for *I. alpestris* with the shortest distance to water as dynamic variable

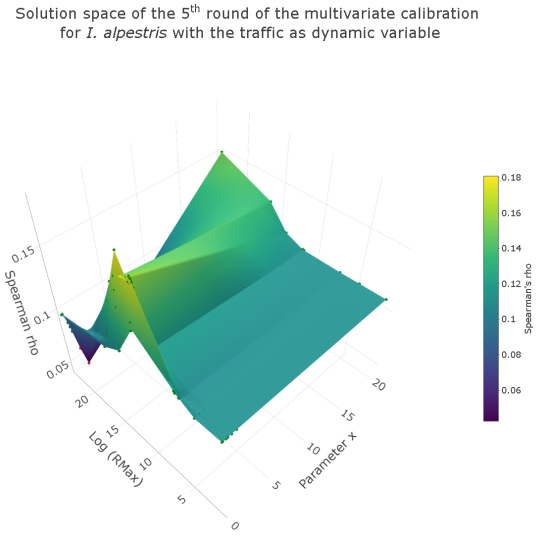

(c) Solution space of the 5^{th} round of the multivariate calibration for *I. alpestris* with the traffic as dynamic variable

Figure 3.1: Examples of solution space patterns in the multivariate calibration

3.4.2 The connectivity and resistance models

Table 3.6 summarizes the optimum parameter sets obtained in the multivariate calibration and the subsequent Spearman's rho yielded by the different connectivity models. The resistance models obtained with these parameter sets are represented in Figure 3.2. The distribution of the resistance of the edges of the network is presented in the histograms of Figure 3.3. In addition, the distribution of the resistance of the edges resulting from each single variable and the combined variables as well as the current of the multivariate connectivity model are summarized in Table C.1 in Appendix C. The maps of resistance induced by the single variables for all five species are also shown in this appendix.

Table 3.6: Summary of the results of the multivariate calibration

Species	Variable	Parameter x	$RMax$	Spearman's rho	S statisitc	P value
B. bufo	Shortest distance to water	70	$1 * 10^{13}$	0.2129	20656207.34	< 0.0001
	Slope	5.5	5			
	Traffic	8.6	500			
E. calamita	Shortest distance to water	40	1000	0.3247	403081.08	< 0.0001
	Slope	10	$1 * 10^{7}$			
	Traffic	20	$1 * 10^{9}$			
H. arborea	Shortest distance to water	30	$1 * 10^{10}$	0.5073	66039.36	< 0.0001
	Slope	13	$1 * 10^{12}$			
	Traffic	0.1	$1 * 10^{5}$			
I. alpestris	Shortest distance to water	17	$1 * 10^{11}$	0.2060	55824817.30	< 0.0001
	Slope	2.6	$1 * 10^{5}$			
	Traffic	0.7	$1 * 10^{6}$			
	Land cover	0.7	1000			
R. temporaria	Shortest distance to water	0.01	$5 * 10^{4}$	0.2205	20457550.96	< 0.0001
	Slope	9	$5 * 10^{6}$			
	Traffic	9	$5 * 10^{6}$			

B. bufo

The multivariate model for *B. bufo* yielded a Spearman's rho of 0.21. The parameter x and $RMax$ for the shortest distance to water were the highest among the variables for this model. This combination lead to a sharp increase of resistance after a threshold distance to water of about 800 m as shown in Figure 3.2 A. For this species, both the slope and the traffic variables had a $RMax$ below 1000 which is low especially compared to the $1 * 10^{13}$ obtained for the shortest distance to water. For those two variables, the parameter x was rather low but still above 1. Overall, these parameter sets resulted in low resistance in most of the edges as can be seen in Figure 3.3.

E. calamita

The multivariate model for *E. calamita* yielded a Spearman's rho of 0.32. The three variables included in this model had a parameter x higher or equal to 10. On the other

hand, the $RMax$ of the shortest distance to water for this species only reached 1000, whereas the slope and the traffic reached $1 * 10^7$ and $1 * 10^9$ respectively. Combined with their respective parameter x, it is clear that the shortest distance to water did not create much resistance compared to the other two variables as shown in Figure 3.2. They, however, created similar levels of resistance with the traffic slightly surpassing the slope. But the distribution of the values of those two variables differ greatly (see the histograms at the top of Figure 3.2) Therefore, the traffic induced a significantly higher resistance than the other variables in only a few edges as can be seen in Figure 3.3. The slope is, therefore, the dominant variable for this species.

H. arborea

H. arborea yielded the best correlation with a Spearman's rho of 0.50. Similarly to the first two species described, parameter x of the shortest distance to water stood out from the other variables with a comparatively high value of 30. However, for this species, the slope yielded the highest $RMax$ followed by the shortest distance to water. The $RMax$ for the traffic was several orders of magnitude smaller but combined with the parameter x below 1, it creates a rather high resistance in all the edges intersecting roads (Figure 3.3). It can also be seen in the almost straight line in create in Figure 3.2 C. Nonetheless, the slope seems to be the dominant variable as it creates a wide range of resistances due to its rather low parameter x of 13. In Figure 3.2 B, one can see that almost the whole range of slope value do induce resistances.

I. alpestris

The model for *I. alpestris* yielded the lowest correlation with 0.21, close to that of *B. bufo*. For this species, both the traffic and the slope have rather low parameter x below 10 but with the traffic being even below 1 which greatly affects the resistance model shown in Figure 3.2 C. Combined with their respective $RMax$ value this results in all the edges having a rather high resistance as shown in Figure 3.2 B and D. Comparatively to the other variables of the model, the shortest distance to water took a relatively high value of parameter x but the difference is not as marked as for the previous two species. Combined with its comparatively really high $RMax$ of $1 * 10^{11}$, this variable also induces resistance in most of the edges. Finally, the land cover yielded similar results as in the univariate calibration with the $RMax$ still significantly lower than for the other variables. This leads in all the edges to have a land cover induced resistance three orders of magnitude lower than what the traffic induced. Overall, for this species, all the variable induced rather high resistances but the shortest distance to water stood out with its even higher $RMax$.

R. temporaria

Finally, the model for *R. temporaria* achieved a Spearman's rho of 0.22. The parameter x for the shortest distance to water stood out for this species as it reached the lowest value overall of 0.01. It is the only species for which this variable does not have the highest parameter x of all variables. When testing parameter sets including a null parameter x, ie. all the edges having a resistance from that variable equal to $RMax$, the correlation saw a sharp decrease but still reached similar values as with the parameter x set to 0.1 or 0.5. This means that this variable induced a resistance really close to the $RMax$ value of $5 * 10^4$ to almost all the edges. The optimum parameter sets identified for the slope and the traffic were the same with a parameter x of 9 and a $RMax$ of $1 * 10^6$. The $RMax$ for the three variables included in this model were, therefore, really similar to each others. When looking at Figure 3.2 and 3.3, one can see that the shortest distance to water sets a benchmark resistance in all the edges that the other variables can barely compete with.

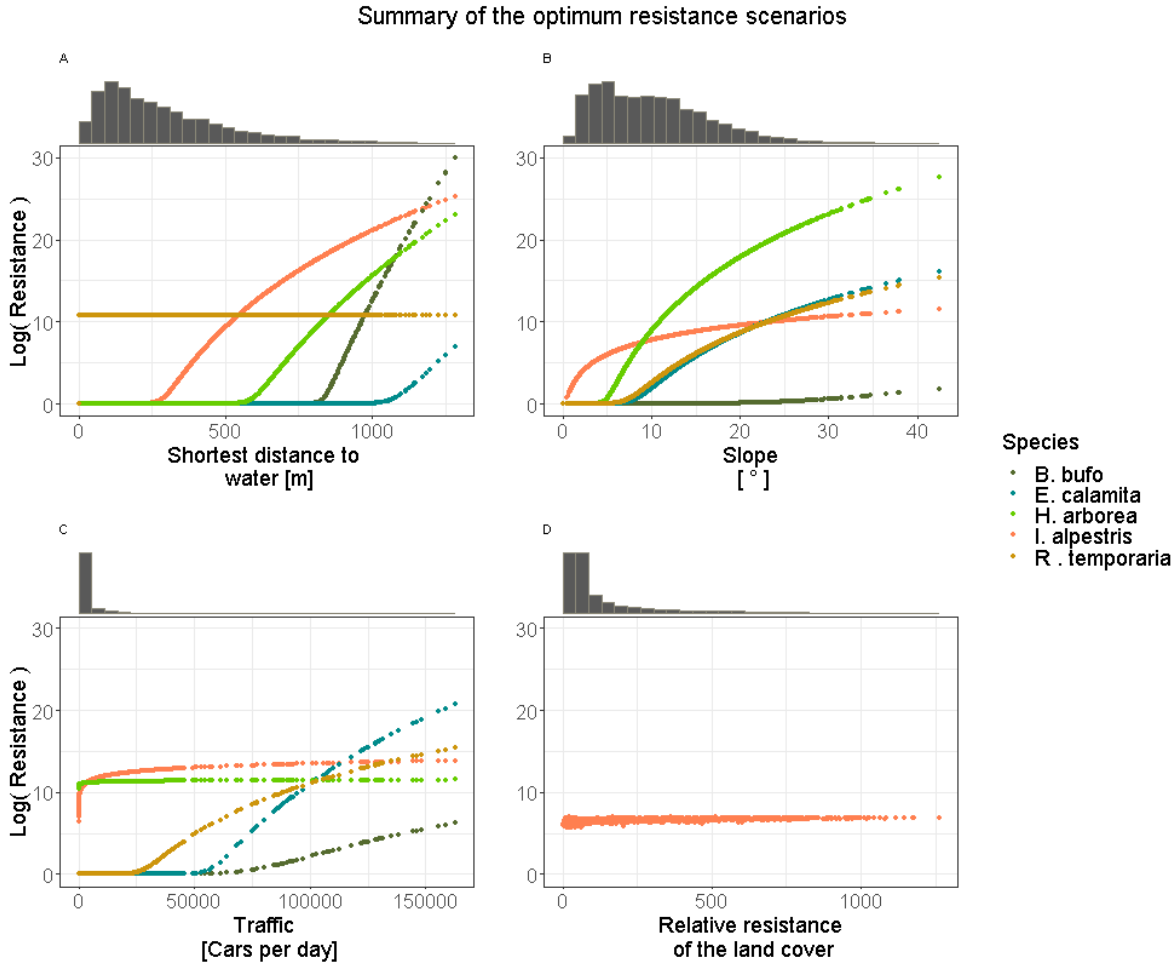

Figure 3.2: Summary of the resistance models included in the final connectivity models. The species are shown in a unique graph for visualisation reasons but the comparison between the results of different species for one variable is risky (see chapter 4.5 for a explanation on this). Note also the logarithmic scale of the y-axis.

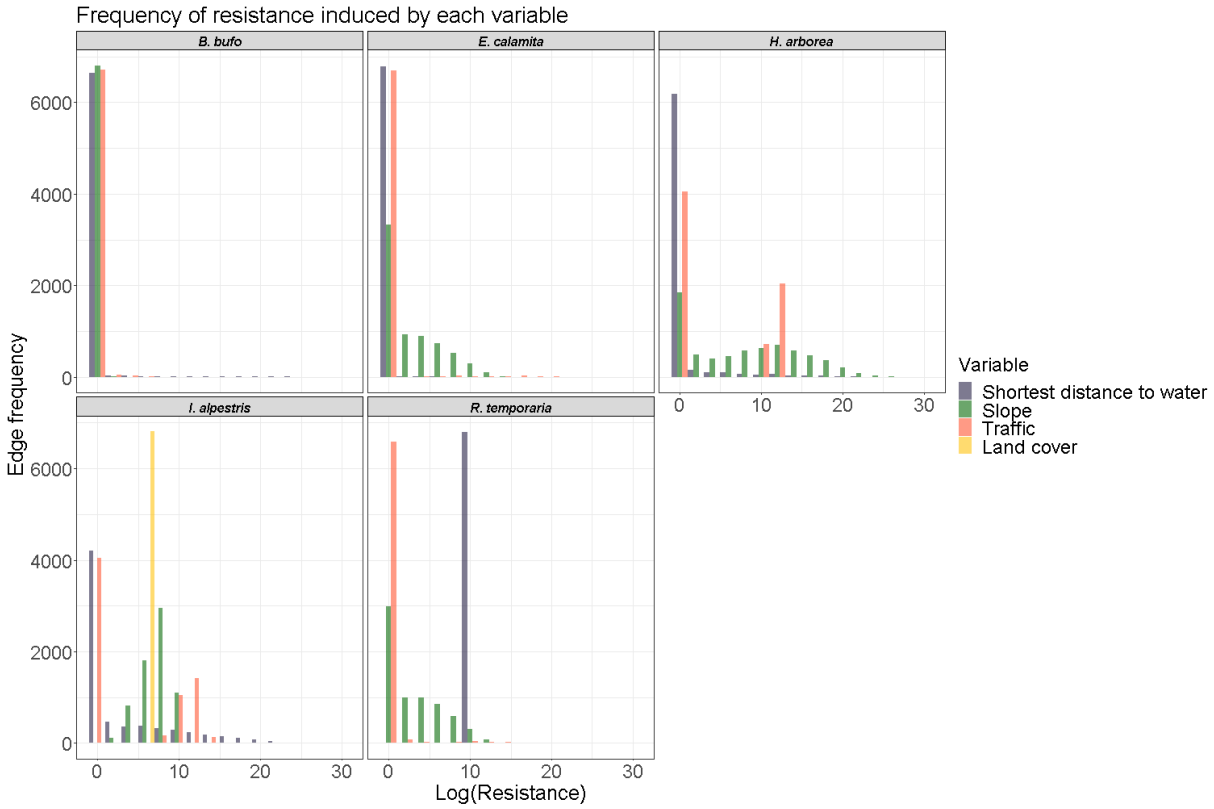

Figure 3.3: Distribution of the resistance induced to the edges by each variable. This figure is to be read with the distribution of the value of the variables themselves in mind (see the histograms of Figure 3.2). The variables for which the parameter x is lower than 1 see their distribution concentrated around the value of the $RMax$ as is the case for the shortest distance to water for *R. temporaria*. The highly skewed values of the traffic explain the two peaks for this variable for *H. arborea* because although the parameter x is below 1, a lot of edges do not have any traffic and consequently have no resistance. The variables with a high $RMax$ and a rather low parameter x see their resistance spread across a wide range of values as is the case for the shortest distance to water for *I. alpestris*. Finally, a peak of low resistance edges will appear if the parameter x is extremely high irrespective of whether the $RMax$ is high or low, or if the $RMax$ is low. *B. bufo* illustrates these cases of figure perfectly.

Chapter 4

Discussion

Connectivity modelling tools like CS rely heavily on the spatial representation of the landscape resistance to animal movement. The resistance at any given point depends on various environmental variables and is specific to every species (Zeller et al. 2012). It is, therefore, impossible to measure it directly. Modelling resistance has thus become a common approach when investigating connectivity (eg. Janin, Léna, Ray, et al. 2009; Graves et al. 2014; Churko et al. 2020). However, some subjectivity remains in the definition of this somewhat esoteric measure, limiting our understanding of its impact on species movement. By implementing a framework first developed by Shirk et al. (2010) and further experimented by Finch et al. (2020) on a network representing various environmental variables, the present study showed the impact of the selection of the resistance model on the final connectivity model for five amphibians species. The shortest distance to water was identified as a dominating factor of connectivity. The slope was also determinant for some of the species. The traffic played a minor role compared to those two variables due to its scattered distribution in the landscape. Finally, no effect of the land-cover could be identified due to a poor representation of its resistance in the network.

4.1 Abundance interpolation

The transformations of the abundance data affected the species unequally but, overall, it did not impact their distribution significantly. This indicates that the interpolated data used for the calibration is still a fair representation of the initial data set. However, the interpolation of the abundance to the nodes of the network did increase the correlation between the connectivity models and the abundance data substantially compared to those obtained with the site average. This is probably due to this representation of the data being a better proxy for the distribution of the species across the landscape. The higher number of nodes which could be selected to calibrate the model after this transformation probably also played a role in this improvement. However, the trade off

of this interpolation is that possible sampling bias in the monitoring data set are likely to have been amplified. A region for which more sampling efforts have been made thus counting more sampling location will have more weight in the interpolated data because a weighted **sum** of the observations at the sampling locations was taken. The inverse is also true for regions with lower sampling efforts.

4.2 Network representation of the environmental variables

The shortest distance to water and the slope were initially in the form of rasters. Because the edges covered the whole study area regularly, taking the mean value around the edges is close to randomly selecting some cells of the raster. Thus, the distribution of those values was barely impacted.

The transposition of the traffic was more impacted because taking the sum increased the range of values which in turn affected the mean and the standard deviation. But because many roads are considered to have really low daily traffic values or zero daily traffic, the original values of the variable were highly skewed and the median was null. Although the transposition slightly reduced the skewness, many edges did not intersect with roads with traffic and obtained null values. Thus, the median stayed null. However, these effects were expected and do not suggest a bias in the representation of the variable in the network.

The land cover suffered the strongest distortion in the transposition. The range of values was only slightly reduced through the transposition, but the mean and the median were significantly reduced in the process proportionally to the initial values. This also appears in the shift of the skewness from negative to positive. This shift is probably explained by the high relative resistance value accorded to the buildings (10). The number of polygon representing buildings was higher than other classes because one of the main purpose of the cadastral map is to accurately represent them, whereas other land cover types are represented in larger therefore less numerous polygons. When transposing the data to the network, I corrected for the area of the polygons decreasing this bias of the buildings which explains the shift of skewness. For this variable, further results showed that the transposition blurred the effect of the resistance model. Furthermore, the values presented in Table 3.3 do not take into account the fact that the relative resistances were transformed by the resistance models before being transposed to the network (step 2.3 in the conceptual model in Figure 2.4 was skipped). Because the resistance models modifies the range of values (min and max), the amplitude of the changes in the indicators observed in Table 3.3 was even greater for the resistance values used in CS (obtained when applying step 2.3, 2.4 and 2.5). An example of this can bee seen in Table C.1 in Appendix C.

Overall, these results show that even though the transposition to the network is a heavy transformation of the data, the patterns of connectivity observed should not be a sole artefact of this transposition. Working with regular grid network therefore seems to be an efficient way of accelerating computation in CS, which in turn allows to work with a high number of species and test many different resistance models. However, it needs to be done with care and the state of the input data needs to be well understood in order to maintain the signal through the whole process as the example of the land cover showed.

4.3 Univariate calibration

The result of the univariate calibration are difficult to interpret as such because many of the variables were limited by the values allowed for both the parameter x and $RMax$. Because the main objective of this calibration was to find a starting point for the multivariate calibration and due to time constraint, it was not further explored. However, I could still identify some trends in this first round of calibration. The main one being that the shortest distance to water was the variable that, alone, best explained the connectivity of the landscape for the five species. This was an expected result due to the semi-aquatic life-cycle of all Swiss amphibians. The slope came second but it was disputed by the traffic for some of the species. This compares with what Cayuela et al. (2020) observed in his review.

The second trend that stood out of this round of calibration was the low explanatory power of the land cover. Even though it is not impossible that the resistance induced by the land cover is not a good variable to explain the connectivity of the landscape for amphibians, published literature suggests otherwise (eg. Stevens, Polus, et al. 2004; Janin, Léna, Deblois, et al. 2012; Covarrubias et al. 2020). As mentioned above, the reason for this apparent absence of effect is probably to look for in the transposition of the landscape information to the network.

Firstly, the values used as input for the resistance model are ranks and therefore already represent an abstraction of the landscape and not a measured value. Furthermore, even though those ranks were established based on a literature review and educated guess on the ecology of the different species, it was not proofed by experts and it is not impossible that mistakes were made.

Secondly, the resistance model was applied before a composite value of these relative resistances was transposed to the edges of the network. This was necessary to try capture the evolution of the resistance between those ranks. However, this damped the effect of the resistance model and probably participated in the lower correlation.

In order to fully understand the role of the land cover for amphibian connectivity, a better way to include it in the model would be to take the percentage of the edges covered

by each class. Each of them would then be calibrated as a separate variable. In that way, the information transposed to the network would be directly measurable. This would also render this type of analysis more independent from expert knowledge to be more objective because no ranking of the land cover classes would be needed. One would only have to determine if a given class favors or hinders the movement of amphibians. However, this would be more time consuming because of the increased number of variables to calibrate.

4.4 Multivariate calibration

4.4.1 The process

Computing the correlation between the current and various sets of absences for the same multivariate resistance model allowed to show that the optimums observed in the two dimension solution space were not artefacts of the absences chosen. The location of the ridges described in chapter 3.4 often did not differ between the absences set, only the peak shifted along that ridge. In fact, when looking at the connectivity maps, little to no differences in the patterns could be observed between the parameter sets composing those ridges. This indicates that the patterns of connectivity observed on the current maps, and thus the connectivity model, should be as close to reality as possible given the current modelling choices even if a mistake was made when selecting the optimum parameter set for the resistance model.

Furthermore, some errors during the calibration forced me to restart it for some species. Due to the complexity of identification of the optimums, the combination of parameters at each round in the second attempt were not always the same as in the first attempt. Nonetheless, after multiple rounds of calibration for the various variables in the model, the same stable optimums for the parameter sets were reached as in the first attempt. This experience reinforced my confidence in the fact that the final resistance models identified do maximise the correlation and that they are not local optimums in the multidimensional solution space.

4.4.2 The connectivity and resistance models

Overall, the resistance induced by the variables and the subsequent connectivity patterns were driven by two main factors: the parameter set and the distribution of the values of the variables. The combination of parameter x and $RMax$ determined both the distribution of the resistance in the edges and the scale of the resistances. However, the distribution of the resistance was also highly impacted by the distribution of the values of the variable themselves because they are at the core of the resistance models. This was particularly blatant for the traffic similarly to what was already observed by Shirk et al.

(2010) when discussing the impact of an interstate Highway in their study. Nonetheless, the influence of the distribution of the values of the variables still let differences between the species appear. This shows the importance of considering species separately when modelling connectivity as already put forward by Cushman (2006).

B.bufo

None of the variables induced a strong resistance for *B. bufo* except the shortest distance to water but only for a limited number of edges (Figure 4.1 (a)). These few edges created the dark green patterns observable in Figure 4.1 (b). The resistance induced by the shortest distance to water in those areas was so high that the current seemed to avoid them altogether which created the high connectivity areas around them by concentrating the current. The influence of the ring of focal nodes is clearly identifiable as with the no variable scenario (see Figure B.2 in appendix B). It is due to the low variation of resistance between the edges but it does not reach the calibration area. These results are coherent with the observation of Sztatecsny et al. (2005) and the fact that this species is rather mobile. They also suggest that the variables chosen here do not play an important role for the connectivity of the landscape for this species at that scale, otherwise stronger patterns would have been observed.

E. calamita

Slope was the dominant variable for this species. This is well reflected in the connectivity map, most of the current was contained within the flat regions (Figure 4.1 (d)). However, high traffic values induced resistance higher than what the slope could reach indicating that busy roads might be barriers for this species. This was also blatant in the connectivity map where the Highway 1 clearly appears in darker green, it is also identifiable in the resistance map in panel (c). Moreover, this strong barrier stopped the current from reaching the focal nodes situated below the Highway resulting in a concentration of current right above it and a lower connectivity area right below the Highway between the villages of Rütihof and Dättwil.

Similarly, Rowe et al. (2000) could show the barrier effect of urban settlements and their associated road network on the gene exchange between populations of this species. The present results also compare to the conclusion of Stevens, Leboulengé, et al. (2006) who argued that the preference of this species for open-land such as roads might lead to a decrease of the effective rate of dispersal due to higher road mortality.

Interestingly, the shortest distance to water played a minor role for the connectivity of this species. It might be explained by the fact that this species relies on temporary water accumulations to breed (KARCH 2020). Those ponds do not appear on the cadastral map and were, therefore, not taken into account here. They are also more likely to form

in flatter regions which also partially explains the importance of the slope.

H. arborea

Slope was the dominant factor for this species as well. However, for this species, the shortest distance to water did play an important role for the connectivity. Because of the dominance of the slope, the patterns resulting from this second variable are only observable in flatter regions where the areas further away from water also show a decrease of connectivity (Figure 4.1 (f)). Finally, the traffic acted as a relatively strong barrier for this species. This was the case for the whole range of daily traffic values as the peak caused by the low parameter x for this variable in Figure 3.3 suggests. In the connectivity and resistance maps, the effect is more difficult to observe because of the combined effect of slope and shortest distance to water but it is observable nonetheless particularly in the same region as for *E. calamita* (the resistance maps of the individual variables in Appendix C better show the impact of the traffic).

Negative effects of roads and traffic on the suitability of the habitat of this species have already been observed multiple times (Pellet, Guisan, et al. 2004; Pellet, Hoehn, et al. 2004) and my results suggest that it might also have an effect on their dispersal. On the other hand, Pellet, Hoehn, et al. (2004) could not see an effect of the distance to the nearest pond on habitat quality. However, some studies showed that patchily distributed ponds facilitated the movement of individuals between breeding sites (Angelone et al. 2009; Le Lay et al. 2015). The present results confirm the findings from the two latter studies. Once again, such complex pond systems are more likely to form in flatter regions which partly explains the importance of the slope.

I. alpestris

For this species, edges located the further away from any water body were subject to extremely higher resistances compared to what the other variables could induce. This lead to low connectivity area patterns visible on the map in Figure 4.1 (h) (dark green spots). This is surprising for this rather mobile species but not totally contradictory. In fact, those low connectivity areas are rather small and leave a lot of space for the individuals to move through because many edges still oppose little resistance. In regions closer to water it was difficult to differentiate between the effect of the other three variables because they all induced resistances in the same range in a large number of edges as shown in the histogram of Figure 3.3. Some patterns could still be observed for some flat valley bottom and the same Highway stretch mentioned above for example (see the resistance maps of the individual variables in Appendix C). This dominance of the shortest distance to water in only a small domain of the distribution of its values hints at a scale effect, where the variable dominating the connectivity patterns at a high scale plays a minor

role at another scale as described for habitat suitability in a case study by Dussault et al. (2005).

The relative high resistances induced by all the variables is surprising for *I. alpestris* and more difficult to explain. Low resistance were expected due to its high vagility for an amphibian, similarly to what was observed for *B. bufo*. It points out at a potential pitfall of the method discussed in chapter 4.5.

Contrary to the results of *H. arborea* and *E. calamita*, the effect of the roads seemed to be more closely linked to the daily traffic values, as shown in Figure 3.3. This variable induced a wider range of resistance for *I. alpestris*. This is due to the parameter x of 0.7 that created an inflexion point in the resistance curve right in the range of traffic values where most roads are found (Figure 3.2 C). Studies looking specifically at the role of roads on the dispersal of *I. alpestris* could not find an effect, which contradicts the present results (Prunier et al. 2014; Luqman et al. 2018). However, this is still disputed in literature (Emaresi et al. 2011).

Finally, the fact that the land cover data results in rather uniform resistances could be an indication that the movement of this species is lightly impacted by this variable. This would be consistent with the vagility of this species. However, these results might just be another sign that the transposition of this variable to the network simply homogenized the relative resistances whipping out its signal.

R. temporaria

For this species, all three variables had really similar $RMax$, thus inducing similar upper values of resistance. However, the extremely low parameter x for the shortest distance to water caused almost all the edges to have a base resistance close to $5 * 10^4$ and made it the determinant variable here. Because the other two variables could induce such resistance in only a few edges, they could only create faint patterns in the connectivity model. They were induced by the highest value of those two variable found in the network such as Highway 1 once again clearly identifiable in Figure 4.1 (i). One example of such faint pattern is the same area of low connectivity below the Highway 1 observed for *E. calamita* and *H.arborea* (Figure 4.1 (j)).The few high connectivity edges (in red) can be explained by the shortest distance to water. Those edges follow the river bed of the Aare and have thus extremely low mean shortest distance to water. They are the few edges for which this variable did not induce high resistance, the current, therefore, concentrate in those edges.

In fact, because of the strong benchmark resistance set by the shortest distance to water, it is almost as if any resistance below it did not have any effect. The resistance in all edges is so similar that the star like patterns of the no variable scenario were identifiable in the South-East quarter of the study area, mostly outside of the calibration area. The

ring of focal nodes is also identifiable (Figure 4.1 (j) and Figure B.2 (b) in Appendix B). Altogether, the landscape appears uniformly connected which is not totally unexpected for this wide spread species even though previous studies could identify some patterns (Decout et al. 2012). The latter study identified the distance to the nearest wetland as a stronger predictor of habitat suitability than the slope for *R. temporaria*, the present results suggest that this might also be true for the connectivity of the landscape. However, because the land cover was dropped of the model none of the variables were related to the presence of forest which played an important role for the connectivity of the landscape in the study of Decout et al. (2012). Including further variables related to forests in the model for this species, such as the percentage of the edges covered by forest, would, therefore, probably result in more pregnant connectivity patterns.

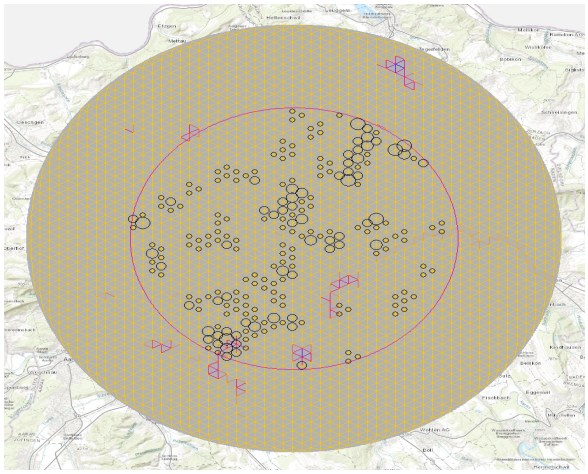

(a) Resistance *B. bufo*

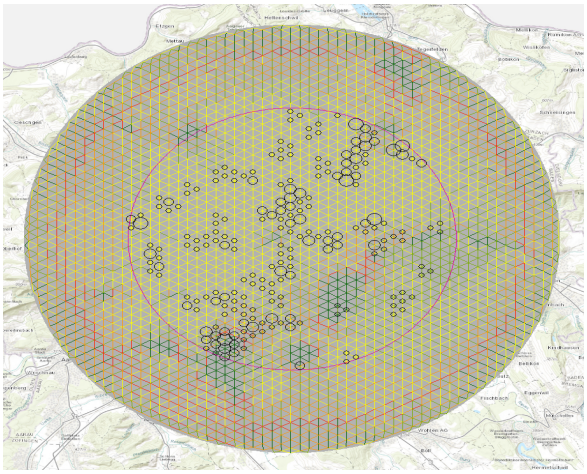

(b) Connectivity *B. bufo*

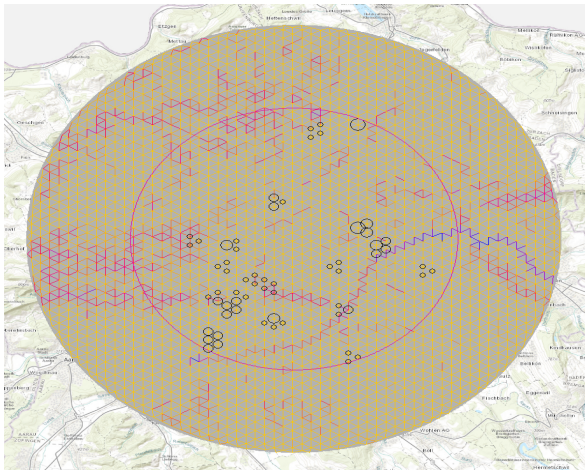

(c) Resistance *E. calamita*

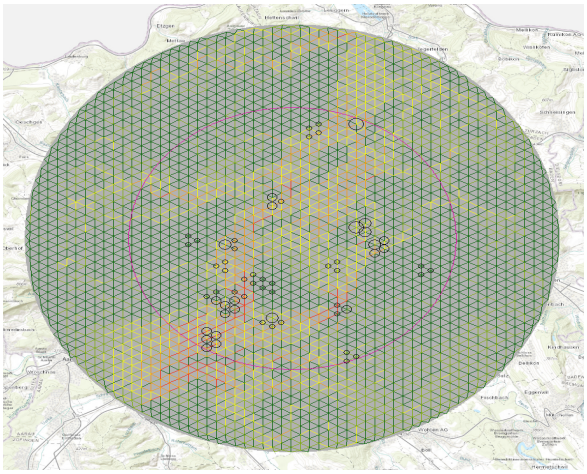

(d) Connectivity *E. calamita*

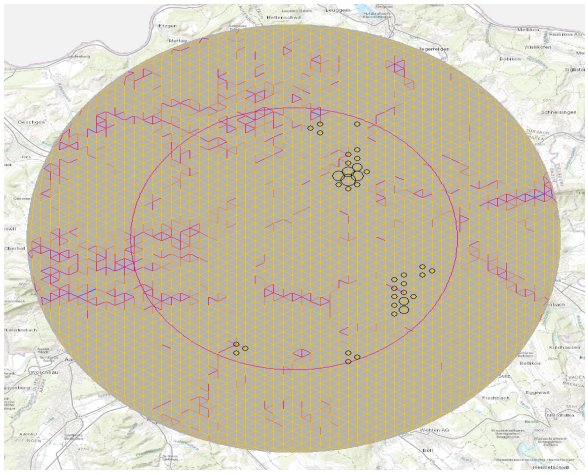

(e) Resistance *H. arborea*

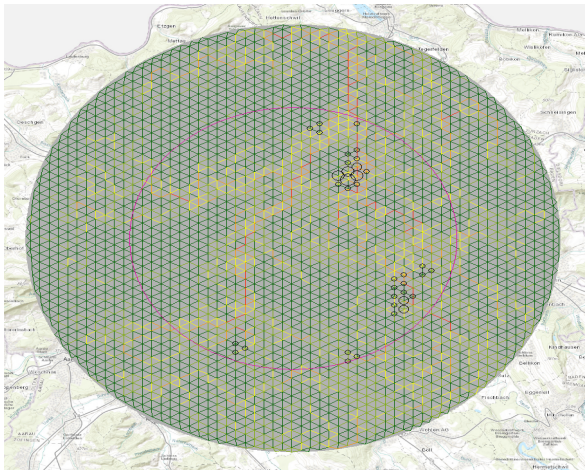

(f) Connectivity *H. arborea*

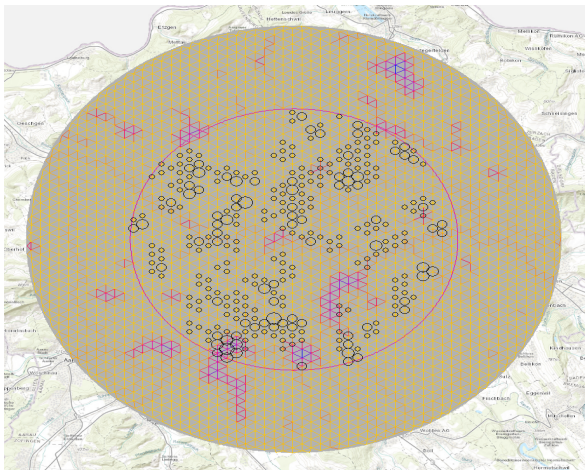

(g) Resistance *I. alpestris*

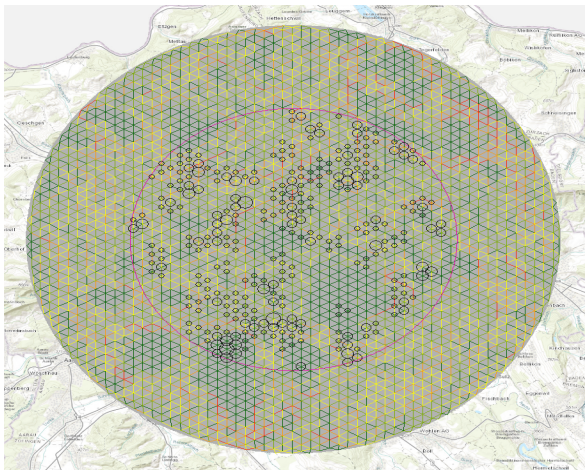

(h) Connectivity *I. alpestris*

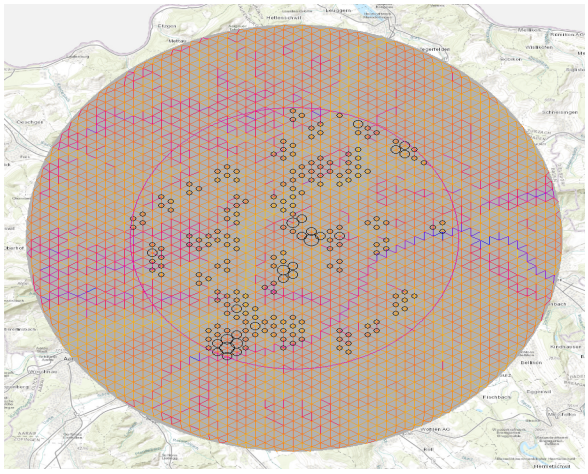

(i) Resistance *R. temporaria*

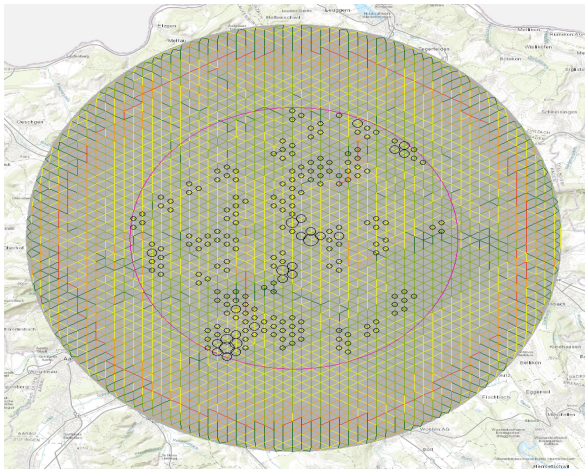

(j) Connectivity *R. temporaria*

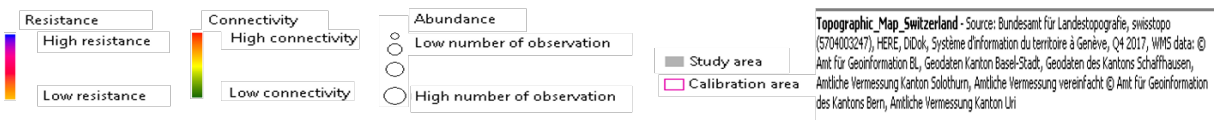

Figure 4.1: Multivariate resistance and connectivity of the landscape for the five study species. Note that the color range is specific to the species.

4.5 Limitations and opportunities of the method

Studying the movement of amphibians is a complex task because of their size, the variety of their movement patterns and because they are often hard to find outside of the breeding season. Various experimental studies have tried to quantify the movement of amphibians but they all came across strong limitations regarding the type of movement observed (migration, dispersal,...) and often focused on a single species (eg. Sinsch 1988; Stevens, Polus, et al. 2004). The method experimented here allowed to produce results comparable with existing literature for five species and therefore has great potential. However, it proved to be tricky sometimes from the implementation to the interpretation of the results and has room for improvement. The next few chapter will hold a critical view on the method and point at further opportunities.

Modelling choices

One has to remember that models are per definition limited by the modelling choices made. The univariate calibration round was a good illustration of that as some of the variables were limited by the range of values allowed for $RMax$. Such bias was already identified as problematic in connectivity analysis by Spear et al. (2010). Similarly, CS also imposed some limitations in the multivariate calibration. When the $RMax$ was really high ($1 * 10^{13}$) and the parameter x low (0.1) for the skewed values of the traffic, it had a hard time computing connectivity because the roads were such high barriers that no current could cross the study area at all. I also postulated that the resistance of the different variables was additive as did Shirk et al. (2010) and Finch et al. (2020) but nothing suggests that there is not more complexity in this relationship. This aspect would also be worth exploring in further studies.

A last example of the limitation of the modelling choices made comes from the equation used to approximate resistance. The chosen equation allowed to model a wide range of relationship between the variable and the resistance as shown in Figure 2.3. However, other approximations might have yielded better results. For example, the relationship between the shortest distance to water and the resistance it caused to *R. temporaria* (Figure 3.2 A) might have been better approximated by a linear function with a vertical displacement of the intercept ($R = Var * x + RMin$). Similarly, a sigmoid curve might have better represented the fact that when an amphibian is found 10 m away from water it actually will have walked a total of 20 m once it has returned to the water. Walking ten meter further away from water will therefore have a proportionally higher impact on the overall effort of the trip and consequently its resistance when starting 10 m away from the water than when starting already 400 m away but will not be really significant when starting from the water. Refining the model to better fit the variable at hand and its

ecological meaning would be another possible improvement. But it is also a Pandora box because finding the perfect model could result in overfitting the calibration data. This was identified by Shirk et al. (2010) as a potential limitations of the framework experimented in this study.

Quality of the input data

A model is always also limited by the quality of the data, mine was no different. One example of that arose from the traffic data set which did not include information on the bridges and underpass that might facilitate amphibian movement. The barrier effect of this variable is, therefore, probably overestimated.

The abundance data presented a few limitations as well. First, because this data set was produced by a citizen science monitoring program, I had no control on how the data was collected. For example, it is likely that it includes sampling bias towards the rarer species it is primarily aimed at or towards newly built ponds more closely monitored. Second, as already mentioned, abundance is not the best predictor of connectivity, especially when acknowledging the scale and the study species considered here. It is impossible for one individual to cross the whole study area even in a life time. Therefore, because of this scale, the type of movement modelled here was dispersal over multiple generations or gene exchange but neither of those two actually relate to abundance directly as mentioned in 2.3.2. In fact, abundance is a predictor of gene exchange due to population dynamics in addition to connectivity (Weckworth et al. 2013; Hague et al. 2016). But the inverse causality (dispersal/gene exchange predicting abundance) seems not to be a good indicator as suggested by Lowe and Allendorf (2010) and is not supported by the existing literature found. I think this scale mismatch partly explains the rather low Spearman's rho obtained by my connectivity models, which under this light appear encouraging. Further studies using this method should try to match the type of fitting data they use to the scale and the movement type they are investigating. Furthermore, by collecting the right data one could differentiate between the movement type of the amphibians, which as seldom been made. One could also look into the movement ecology of other taxa.

Limited comparability

This method allows for the comparison of:

- The resistance induced by the different variables for one species.
- The relative importance of the variables in the multivariate resistance models between the species.

However, the comparison of the resistance caused by one variable with the resistance of that variable for another species is risky. This is the pitfall mentioned in 4.4.2 for *I.*

alpestris and I will use this example to illustrate it. I believe that the relatively high resistance induced by all the variables for this species might be related to the fact that the current going through each edge in CS is defined by its resistance **relative** to that of the surrounding edges. Therefore, when calibrating one variable, the model was pushed to match the resistance of the static variables in order to fit the patterns reflected in the calibration data. For *I. alpestris*, the parameter x and the $RMax$ for the shortest distance to water created a relatively high resistance in a high number of edges in order for the pattern of connectivity it drives to be best expressed in the connectivity model. Because of that, the other variables had to match this range of resistance in order for the pattern that **they** imply to be identified when computing the correlation. But when calibrating the slope for *B. bufo* for example, it did not have to match the same high base resistance from the shortest distance to water to express its patterns. Therefore, the comparison of the resistance of the slope between the two species directly might lead to misinterpretations.

The high resistance observed for *I. alpestris* and *R. temporaria* might just be a sign that the faint patterns related to the chosen variables are better expressed with a wide range of resistance values (middle to low parameter x and high $RMax$) than a small one. The scale of these resistances would, therefore, likely change if a variable implying stronger patterns of connectivity, and therefore better explaining it, was introduced in the multivariate resistance model but their relative importance probably would not. This calls for a cautious interpretation of the results of such models. A fine selection of variable included in the model is also crucial (Beier et al. 2008; Zeller et al. 2012). A confirmation by field studies might help anchor these results to allow comparison. One could also imagine normalizing the resistance against measured data or the value of one of the species to allow for easier inter-species comparison but such a transformation would have to be done with extreme care.

Transferability of the models

Because the resistance models made use of the maximum value found for one variable in the study area, the results might not be transferable to other locations as this maximum value might change. However, Finch et al. (2020), who used the same calibration method to investigate the connectivity of the network for commuting bats around roosting trees, could transfer their final resistance models to other roosting trees without substantial loss of correlation in the connectivity model. It is therefore important to carry out the necessary sensitivity analysis before generalizing the results of this method.

As mentioned in the discussion of the results of *I. alpestris* (chapter 4.4.2), the variables dominating resistance at one scale might not play the same role at a smaller or bigger scale. The resistance model is, therefore, not directly transferable across scales. Dussault

et al. (2005) illustrated the same limitation in habitat suitability modelling. Ideally, one should study connectivity at a few different scales significant for the study species to be able to draw better conclusion on the role of a given variable for overall connectivity (Grand et al. 2003; Cushman 2006).

On the other hand, the similarities between the representation of rasters in CS and the network used suggest that, once calibrated, the resistance model could be applied to the same variables represented in rasters over the same area and run through CS one last time in order to obtain a better resolution for the connectivity. This would require further comparison with the calibration data but would consist in another sensitivity analysis and give another perspective on the robustness of the results. A better resolution would also be of greater value for local conservation authorities.

Computation time

Even though networks were used instead of rasters to increase the computation speed, it remained a limiting factor regarding the number of resistance model tested. Switching to the newer version of CS in the new language *Julia* would probably improve this (Anantharaman et al. 2019). Furthermore, making use of machine learning process to optimize the selection of the model to test in both calibrations would really bring this method to another level and allow to investigate even more variables. Additionally, it could allow to get rid of the lengthy iterative multivariate calibration by calibrating all variables at once.

Chapter 5

Conclusion and outlook

Simplifying the landscape in a network over a small study area allowed me to calibrate a high number of resistance models by analysing the connectivity patterns they underlie. I could identify the parameter sets for the resistance models that generated a best fit between the subsequent connectivity models and interpolated abundance data. The resistance of the variables was first modelled for single variables. This was then used as a starting point for the calibration of multivariate resistance models in a similar fashion. The whole process was completed in a relatively short time span for five Swiss amphibian species and four environmental variables. By analysing the optimum parameter sets obtained by each variable in the multivariate resistance models, the role each of them play for the study species and their relative importance for landscape connectivity could be explored.

I could show that the shortest distance to water is the variable that had the most influence on the connectivity of the landscape overall but some species did not rely on it as much as others. Slope was the second most important variable in determining the landscape connectivity but again species specificity made it the dominant factor for some of them. Finally, the traffic was often the least influential variable due to its uneven distribution in the landscape. However, I was still able to observe some pattern it induced indicating it might be more important at a finer scale. On the other hand, the attempt at including the land cover in a state of the art approach combined with the network approach failed to produce viable results. From this, one can learn the importance of carefully transposing the landscape data to the network and adapting the process to the data type when using this method. I suggest transposing the land cover to the network by looking at the percentage of the edges covered by each land cover class would yield better results and free the method from the subjective evaluation of the expert knowledge.

Not only did my results compare well with existing literature on amphibian movement but this method allowed to get information on the resistance of the landscape for more species at once than previously achieved. I suggest that providing the right calibration

data, one could dive into the different types of movement specific to amphibians (migration, dispersal and home range movement), a differentiation seldom made until now due to the complexity of the task when approached experimentally. Furthermore, even though the method was applied here to amphibians it could be easily used on other organisms or at different scales. Whether the model obtained could later be applied directly to a raster to regain the resolution lost when transposing the data to a network still remains to be answered. Combined with the ongoing innovations in the machine learning domain, the method could be further improved and allow to go a step further in modelling landscape resistance and connectivity.

Altogether, when one considers the general caveats of all models, this methods offers good opportunities serving connectivity modelling purpose in the broader scope of blue-green infrastructure development.

Bibliography

Anantharaman, Ranjan et al. (2019). *Circuitscape in Julia: High Performance Connectivity Modelling to Support Conservation Decisions*.

Angelone, Sonia and Rolf Holderegger (2009). "Population genetics suggests effectiveness of habitat connectivity measures for the European tree frog in Switzerland". In: *Journal of Applied Ecology* 46.4, pp. 879–887. DOI: 10.1111/j.1365-2664.2009.01670.x.

Bach, Peter M. et al. (2015). "Revisiting land use classification and spatial aggregation for modelling integrated urban water systems". In: *Landscape and Urban Planning* 143, pp. 43–55. DOI: 10.1016/j.landurbplan.2015.05.012.

Bach, Peter M., David T. McCarthy, and Ana Deletic (2015). "Can we model the implementation of water sensitive urban design in evolving cities?" In: *Water Science and Technology* 71.1, pp. 149–156. DOI: 10.2166/wst.2014.464.

Bar-David, Shirli et al. (2007). "Long-distance movements by fire salamanders (Salamandra infraimmaculata) and implications for habitat fragmentation". In: *Israel Journal of Ecology and Evolution* 53.2, pp. 143–159. DOI: 10.1080/15659801.2007.10639579.

Beier, Paul, Daniel R. Majka, and Wayne D. Spencer (2008). "Forks in the road: Choices in procedures for designing wildland linkages". In: *Conservation Biology* 22.4, pp. 836–851. DOI: 10.1111/j.1523-1739.2008.00942.x.

Bühler, Christoph (2019). *Amphibienmonitoring Aargau 2019 Methodenbeschrieb*.

Catenazzi, Alessandro (2015). "State of the World's Amphibians". In: *The Annual Review of Environment and Resources* 40, pp. 91–119. DOI: 10.1146/annurev-environ-102014-021358.

Cayuela, Hugo et al. (2020). "Determinants and consequences of dispersal in vertebrates with complex life-cycles: a review of pond-breeding amphibians". In: *The Quarterly Review of Biology* 95.1, pp. 1–36. DOI: 10.1086/707862.

Chandra, Ashok K. et al. (1996). "The electrical resistance of a graph captures its commute and cover time". In: *Computational complexity* 6, pp. 312–340. DOI: i016-3328/97/040312-29.

Churko, Gregory, Felix Kienast, and Janine Bolliger (2020). "A multispecies assessment to identify the functional connectivity of amphibians in a human-dominated landscape". In: *ISPRS International Journal of Geo-Information* 9.5. DOI: 10.3390/ijgi9050287.

Clauzel, Céline, Xavier Girardet, and Jean-Christophe Foltête (2013). "Impact assessment of a high-speed railway line on species distribution: Application to the European tree frog (Hyla arborea) in Franche-Comté". In: *Journal of Environmental Management* 127, pp. 125–134. DOI: 10.1016/j.jenvman.2013.04.018.

Covarrubias, S., C. González, and C. Gutiérrez-Rodríguez (2020). "Effects of natural and anthropogenic features on functional connectivity of anurans: a review of landscape genetics studies in temperate, subtropical and tropical species". In: *Journal of Zoology*. DOI: 10.1111/jzo.12851.

Cushman, Samuel A. (2006). "Effects of habitat loss and fragmentation on amphibians: A review and prospectus". In: *Biological Conservation* 128.2, pp. 231–240. DOI: 10.1016/j.biocon.2005.09.031.

Decout, Samuel et al. (2012). "Integrative approach for landscape-based graph connectivity analysis: A case study with the common frog (Rana temporaria) in human-dominated landscapes". In: *Landscape Ecology* 27.2, pp. 267–279. DOI: 10.1007/s10980-011-9694-z.

Doyle, Peter G. and J. Laurie Snell (2000). *Random walks and electric networks*. Ed. by Mathematical Association of America. Washigton, D.C., USA. ISBN: 9781614440222. DOI: 10.5948/UPO9781614440222.

Dussault, Christian et al. (2005). "Linking moose habitat selection to limiting factors". In: *Ecography* 28.5, pp. 619–628. DOI: 10.1111/j.2005.0906-7590.04263.x.

Emaresi, Guillaume et al. (2011). "Landscape genetics of the Alpine newt (Mesotriton alpestris) inferred from a strip-based approach". In: *Conservation Genetics* 12.1, pp. 41–50. DOI: 10.1007/s10592-009-9985-y.

ESRI (2008). *ArcGIS Desktop*. Redlands, CA.

Finch, Domhnall et al. (2020). "Modelling the functional connectivity of landscapes for greater horseshoe bats Rhinolophus ferrumequinum at a local scale". In: *Landscape Ecology* 35.3, pp. 577–589. DOI: 10.1007/s10980-019-00953-1.

Frei, Manuel et al. (2016). "Combining landscape genetics, radio-tracking and long-term monitoring to derive management implications for Natterjack toads (Epidalea calamita) in agricultural landscapes". In: *Journal for Nature Conservation* 32, pp. 22–34. DOI: 10.1016/j.jnc.2016.04.002.

Godet, Claire and Céline Clauzel (2020). "Comparison of landscape graph modelling methods for analysing pond network connectivity". In: *Landscape Ecology*. DOI: 10.1007/s10980-020-01164-9.

Grand, Joanna and Samuel A. Cushman (2003). "A multi-scale analysis of species-environment relationships: breeding birds in a pitch pine-scrub oak (Pinus rigida-

Quercus ilicifolia) community". In: *Biological conservation* 112, pp. 307–317. DOI: 10.1016/S0006-3207(02)00323-3.

Graves, Tabitha et al. (2014). "Estimating landscape resistance to dispersal". In: *Landscape Ecology* 29.7, pp. 1201–1211. DOI: 10.1007/s10980-014-0056-5.

Hague, M. T.J. and E. J. Routman (2016). "Does population size affect genetic diversity? A test with sympatric lizard species". In: *Heredity* 116.1, pp. 92–98. DOI: 10.1038/hdy.2015.76.

Hijmans, Robert J. (2020). *raster: Geographic Data Analysis and Modeling*. R package version 3.3-13. URL: https://CRAN.R-project.org/package=raster.

Janin, Agnès, Jean-Paul Léna, Sandrine Deblois, et al. (2012). "Use of Stress-Hormone Levels and Habitat Selection to Assess Functional Connectivity of a Landscape for an Amphibian". In: *Conservation Biology* 26.5, pp. 923–931. DOI: 10.1111/j.1523-1739.2012.01910.x.

Janin, Agnès, Jean-Paul Léna, Nicolas Ray, et al. (2009). "Assessing landscape connectivity with calibrated cost-distance modelling: Predicting common toad distribution in a context of spreading agriculture". In: *Journal of Applied Ecology* 46.4, pp. 833–841. DOI: 10.1111/j.1365-2664.2009.01665.x.

Joly, Pierre, Claire Morand, and Aurélie Cohas (2003). "Habitat fragmentation and amphibian conservation: Building a tool for assessing landscape matrix connectivity". In: *Comptes Rendus - Biologies* 326, pp. 132–139. DOI: 10.1016/s1631-0691(03)00050-7.

Justen, Andreas et al. (2017). *Modelletablierung Nationales Personenverkehrsmodell (NPVM) 2017*. Tech. rep. Bundesamt für Raumentwicklung (ARE).

KARCH (2020). *Amphibiens de Suisse*. URL: http://www.karch.ch/karch/Especes_amphibiens (visited on 03/26/2021).

Koen, Erin L., Jeff Bowman, Carrie Sadowski, et al. (2014). "Landscape connectivity for wildlife: Development and validation of multispecies linkage maps". In: *Methods in Ecology and Evolution* 5.7, pp. 626–633. DOI: 10.1111/2041-210X.12197.

Koen, Erin L., Jeff Bowman, and Aaron A. Walpole (2012). "The effect of cost surface parameterization on landscape resistance estimates". In: *Molecular Ecology Resources* 12.4, pp. 686–696. DOI: 10.1111/j.1755-0998.2012.03123.x.

Kovar, Roman et al. (2009). "Spring migration distances of some Central European amphibian species". In: *Amphibia-Reptilia* 30.3, pp. 367–378. DOI: 10.1163/156853809788795236.

Le Lay, Gwenaëlle et al. (2015). "Increasing Pond Density to Maintain a Patchy Habitat Network of the European Treefrog (Hyla arborea)". In: *Journal of Herpetology* 49.2, pp. 217–221. DOI: 10.1670/13-056.

Lowe, Winsor H. and Fred W. Allendorf (2010). "What can genetics tell us about population connectivity?" In: *Molecular Ecology* 19.15, pp. 3038–3051. DOI: 10.1111/j.1365-294X.2010.04688.x.

Lowe, Winsor H., Gene E. Likens, et al. (2006). "Linking direct and indirect data on dispersal: Isolation by slope in a headwater stream salamander". In: *Ecology* 87.2, pp. 334–339. DOI: 10.1890/05-0232.

Luqman, Hirzi et al. (2018). "No distinct barrier effects of highways and a wide river on the genetic structure of the Alpine newt (Ichthyosaura alpestris) in densely settled landscapes". In: *Conservation Genetics* 19.3, pp. 673–685. DOI: 10.1007/s10592-018-1046-y.

Martensen, Alexandre C. et al. (2012). "Associations of Forest Cover, Fragment Area, and Connectivity with Neotropical Understory Bird Species Richness and Abundance". In: *Conservation Biology* 26.6, pp. 1100–1111. DOI: 10.1111/j.1523-1739.2012.01940.x.

Mazerolle, Marc J., Matthieu Huot, and Mireille Gravel (2005). "Behavior of amphibians on the road in response to car traffic". In: *Herpetologica* 61.4, pp. 380–388. DOI: 10.1655/04-79.1.

McRae, Brad H. et al. (2008). "Using circuit theory to model connectivity in ecology, evolution, and conservation". In: *Ecology* 89.10, pp. 2712–2724. DOI: 10.1890/07-1861.1.

McRae, Brad H. (2006). "Isolation by resistance". In: *Evolution* 60.8, pp. 1551–1561. DOI: 10.1111/j.0014-3820.2006.tb00500.x.

McRae, Brad H. and Paul Beier (2007). "Circuit theory predicts gene flow in plant and animal populations". In: *PNAS* 104.50, pp. 19885–19890. DOI: 10.1073/pnas.0706568104.

Miaud, Claude, Delfi Sanuy, and Jean-Noël Avrillier (2000). "Terrestrial movements of the natterjack toad Bufo calamita (Amphibia, Anura) in a semi-arid, agricultural landscape". In: *Amphibia-Reptilia* 21.3, pp. 357–369. DOI: 10.1163/156853800507426.

Pazúr, Robert et al. (2021a). "A national extent map of cropland and grassland for Switzerland based on Sentinel-2 data". In: *Earth System Science Data Discussions* 2021. [*in review*], pp. 1–14. DOI: 10.5194/essd-2021-60.

— (2021b). *Cropland and grassland map of Switzerland based on Sentinel-2 data*. DOI: 10.16904/envidat.205. URL: https://www.envidat.ch/dataset/cropland-and-grassland-map-of-switzerland-based-on-sentinel-2-data (visited on 11/05/2020).

Pebesma, Edzer (2018). "Simple Features for R: Standardized Support for Spatial Vector Data". In: *The R Journal* 10.1, pp. 439–446. DOI: 10.32614/RJ-2018-009.

Pellet, Jérôme, Antoine Guisan, and Nicolas Perrin (2004). "A Concentric Analysis of the Impact of Urbanization on the Threatened European Tree Frog in an Agricultural Landscape". In: *Conservation Biology* 18.6, pp. 1599–1606. DOI: 10.1111/j.1523-1739.2004.0421a.x.

Pellet, Jérôme, Sophie Hoehn, and Nicolas Perrin (2004). "Multiscale determinants of tree frog (Hyla arborea L.) calling ponds in western Switzerland". In: *Biodiversity and Conservation* 13, pp. 2227–2235. DOI: 10.1023/B:BIOC.0000047904.75245.1f.

Pittman, Shannon E., Michael S. Osbourn, and Raymond D. Semlitsch (2014). "Movement ecology of amphibians: A missing component for understanding population declines". In: *Biological Conservation* 169, pp. 44–53. DOI: 10.1016/j.biocon.2013.10.020.

Popescu, Viorel D. and Malcolm L. Hunter (2011). "Clear-cutting affects habitat connectivity for a forest amphibian by decreasing permeability to juvenile movements". In: *Ecological Applications* 21.4, pp. 1283–1295. DOI: 10.1890/10-0658.1.

Prunier, Jérôme G. et al. (2014). "A 40-year-old divided highway does not prevent gene flow in the alpine newt Ichthyosaura alpestris". In: *Conservation Genetics* 15.2, pp. 453–468. DOI: 10.1007/s10592-013-0553-0.

R Core Team (2019). *R: A Language and Environment for Statistical Computing*. R Foundation for Statistical Computing. URL: https://www.R-project.org/.

Rae, Charlene, Kristina Rothley, and Suzana Dragicevic (2007). "Implications of error and uncertainty for an environmental planning scenario: A sensitivity analysis of GIS-based variables in a reserve design exercise". In: *Landscape and Urban Planning* 79.3-4, pp. 210–217. DOI: 10.1016/j.landurbplan.2006.01.001.

Rayfield, Bronwyn, Marie J. Fortin, and Andrew Fall (2010). "The sensitivity of least-cost habitat graphs to relative cost surface values". In: *Landscape Ecology* 25.4, pp. 519–532. DOI: 10.1007/s10980-009-9436-7.

Rayfield, Bronwyn, David Pelletier, et al. (2016). "Multipurpose habitat networks for short-range and long-range connectivity: A new method combining graph and circuit connectivity". In: *Methods in Ecology and Evolution* 7.2, pp. 222–231. DOI: 10.1111/2041-210X.12470.

Reh, W and A Seitz (1990). "The Influence of Land Use on the Genetic Structure of Populations of the Common Frog Rana temporaria". In: *Biological Conservation* 54, pp. 239–249.

Reid, Walter et al. (2005). *Millenium Ecosystem Assessment Synthesis Report*. Ed. by Island Press. Washington, DC. ISBN: 1-59726-040-1.

Rosenberg, Daniel K., Barry R. Noon, and E Charles Meslow (1997). "Biological Corridors: Form, Function, and Efficacy". In: *BioScience* 47.10, pp. 677–687.

Rowe, G et al. (2000). "A microsatellite analysis of natterjack toad, Bufo calamita, metapopulations". In: *OIKOS* 88.3, pp. 641–651. DOI: 10.1034/j.1600-0706.2000.880321.x.

Schmidt, Peter et al. (2006). "Dispersal of Triturus alpestris and T. vulgaris in agricultural landscapes – comparing estimates from allozyme markers and capture-mark-recapture analysis Peter". In: Herpetologia Bonnensis II. Pp. 139–143.

Schulte, Ulrich, Daniel Küsters, and Sebastian Steinfartz (2007). "A PIT tag based analysis of annual movement patterns of adult fire salamanders (Salamandra salamandra) in a Middle European habitat". In: *Amphibia Reptilia* 28.4, pp. 531–536. DOI: 10.1163/156853807782152543.

Shirk, A J. et al. (2010). "Inferring landscape effects on gene flow: A new model selection framework". In: *Molecular Ecology* 19.17, pp. 3603–3619. DOI: 10.1111/j.1365-294X.2010.04745.x.

Sinsch, Ulrich (1988). "Seasonal changes in the migratory behaviour of the toad Bufo bufo: direction and magnitude of movements". In: *Oecologia* 76, pp. 390–398. DOI: 10.1007/BF00377034.

Spear, Stephen F. et al. (2010). "Use of resistance surfaces for landscape genetic studies: Considerations for parameterization and analysis". In: *Molecular Ecology* 19.17, pp. 3576–3591. DOI: 10.1111/j.1365-294X.2010.04657.x.

Stevens, Virginie M., Éric Leboulengé, et al. (2006). "Quantifying functional connectivity: Experimental assessment of boundary permeability for the natterjack toad (Bufo calamita)". In: *Oecologia* 150.1, pp. 161–171. DOI: 10.1007/s00442-006-0500-6.

Stevens, Virginie M., Emmanuelle Polus, et al. (2004). "Quantifying functional connectivity: experimental evidence for patch-specific resistance in the Natterjack toad (Bufo calamita)". In: *Landscape Ecology* 19, pp. 829–842. DOI: 10.1007/s10980-005-0166-1.

swissTLM 3D (2015). *Vectorized National Map 1:25'000, Bundesamt für Landestopographie*. Switzerland.

Sztatecsny, M and R Schabetsberger (2005). "Into thin air: Vertical migration, body condition, and quality of terrestrial habitats of alpine common toads, Bufo bufo". In: *Canadian Journal of Zoology* 83.6, pp. 788–796. DOI: 10.1139/Z05-071.

Trochet, Audrey et al. (2019). "Influence of substrate types and morphological traits on movement behavior in a toad and newt species". In: *PeerJ* 6.e6053, pp. 1–17. DOI: 10.7717/peerj.6053.

Uezu, Alexandre, Jean P. Metzger, and Jacques M. Vielliard (2005). "Effects of structural and functional connectivity and patch size on the abundance of seven Atlantic Forest bird species". In: *Biological Conservation* 123.4, pp. 507–519. DOI: 10.1016/j.biocon.2005.01.001.

Vermessungsamt des Kantons Aargau (2020). *AV: Daten der Amtliche Vermessung*.

Weckworth, Byron V. et al. (2013). "Preferred habitat and effective population size drive landscape genetic patterns in an endangered species". In: *Proceedings of the Royal Society: Biological Sciences* 280, pp. 1–9. DOI: 10.1098/rspb.2013.1756.

Westgate, Martin J., Don A. Driscoll, and David B. Lindenmayer (2012). "Limited influence of stream networks on the terrestrial movements of three wetland-dependent frog species". In: *Biological Conservation* 153, pp. 169–176. DOI: 10.1016/j.biocon.2012.04.030.

Zeller, Katherine A., Kevin McGarigal, and Andrew R. Whiteley (2012). "Estimating landscape resistance to movement: A review". In: *Landscape Ecology* 27.6, pp. 777–797. DOI: 10.1007/s10980-012-9737-0.

Appendix A: Reclassification of the cadastral map data

A.1 Reclassifying choices

Reclassifying the cadastral map demanded to make some assumptions on the resistance of each of the original classes. Here, I will explain the main decisions taken in order to make this process as transparent as possible. Table A.1 summarizes the exact composition of each class, whereas table A.2 presents the relative resistance attributed to each new class for each species and the literature justifying these relative resistances. Because the early results of the univariate calibration made it clear that the land cover as included in the model would not give informative results, no further research was made to justify the choices made. This explains the lack of literature for some of the classes.

Buildings

The building class is composed of all the elements that would not allow the movement of amphibians at all. Therefore, cliffs were included in this class because I hypothesized the effect of a cliff or a building would be similar.

Only parts of the objects described in the layer "single object" (Einzelobjekt) were taken into account. Most of them consists of human made structure such as wall, tours and so on and were thus included in the building class. Most however, were deemed insignificant like building details and crucifix or irrelevant for amphibian movement like sources, ski lifts and underground garage. They were thus ignored. The cadastral map also contains a layer representing linear elements. It was not taken into consideration because in the process of transposing the data to the network edges, the surface is used to modify the resistance value. Line having no surface their effect would have been null. Moreover, most of those lines are irrelevant for amphibian movement (eg. electric lines, location of railway line center, etc.)

Road and sealed surfaces

The Road and sealed surface class represents all impermeable surface transformed by men. Because the model also includes a variable about traffic, the relative resistance

considered here is only that of the surface itself. To that the sealed reservoirs were added because they have often sharp banks hindering amphibian movement but were not deemed as impermeable as buildings.

Wetlands

The wetland class regroups all semi-aquatic elements. The difference of resistance between this class and the water conductive class is probably insignificant in some places

Conductive and barrier water elements

The differentiation between conductive and barrier water element has already been discussed in chapter 2.4.4 and will therefore not be further explained here.

Intensively used open-land

The intensively used open-land was created to explore the role of surfaces that have been transformed by human activities but are still expected to allow the movement of amphibians such as gardens and golf courses. It is similar to what Koen, Bowman, and Walpole (2012) tried to represent.

Forest

The forest class is trivial. The inclusion of further data to discriminate between types of forest was considered at some point but left out to avoid adding complexity. It would be interesting for some of the study species as suggested in chapter 4.5.

Sand and gravel pits

The sand and gravel pit class was created because it seemed they are particularly important for some of the amphibian species (KARCH 2020). However, its relative resistance was sometimes hard to assess for some of the species for which it is not really relevant. This also explains the lack of scientific evidence for its position in the table A.2.

Arable land and pastures

The differentiation between arable land and pastures has already been discussed in section 2.4.4. However, the vineyards were added to the arable land class because they are often dry and heavily treated so I estimated the resistance would be similar. On the contrary, the orchards mostly have grass between the trees but are still heavily managed. I hypothesized that the resistance for amphibians of that type of land cover should be close to that of pastures.

Table A.1: Reclassification of the classes of the cadastral map to approximately those of Churko et al. (2020) and from an amphibian movement point of view

Reclassification of the cadastral map					
New class	Churko equilavent	Original class	Description	Source layer	Further comments
Buildings	Settlements	Gebaeude	Buildings	Bodenbedeckung	
		vegetationlos.Fels	Cliff	Bodenbedeckung	
		Mauer	Wall	Einzelobjekt	
		Pfeiler	Pfeiler	Einzelobjekt	
		Unterstand	Outside cover	Einzelobjekt	
		Aussichturm	Observation tower	Einzelobjekt	
		Schwelle	Artificial waterfall	Einzelobjekt	
		Massiver_Sockel	Massiv anchor	Einzelobjekt	
		Ruine _archaeologis-ches_Objekt	Ruines	Einzelobjekt	
		Bahnsteig	Train platform	Einzelobjekt	

New class	Churko equilavent	Original class	Description	Source layer	Further comments
Roads and sealed surfaces	Major roads + Paths and minor roads	befestigt.Bahn	Train tracks	Bodenbedeckung	
		befestigt.Flugplatz	Air field	Bodenbedeckung	
		befestigt.Strasse_weg	Roads and paths	Bodenbedeckung	
		befestigt.Trottoir	Sidewalk	Bodenbedeckung	
		befestigt.Verkehrsinsel	Roundabout	Bodenbedeckung	
		befestigt.Wasserbecken	Sealed water reservoirs	Bodenbedeckung	
		befestigt.uebrige_befetigte	Mixed sealed surface	Bodenbedeckung	
		vegetationslos.Abbau_Deponie	Depot	Bodenbedeckung	
Wetlands	Wetlands	Gewaesser.Schilfguertel	Reed belt	Bodenbedeckung	
		humusiert._Hoch_Flachmoor	Wetlands	Bodenbedeckung	
Water conductiv and barrier	Rivers and lakes	Gewaesser.fliessendes	Flowing water	Bodenbedeckung	This groups was further split see 2.4
Water conductiv and barrier		Gewaesser.stehendes	Static water	Bodenbedeckung	

New class	Churko equilavent	Original class	Description	Source layer	Further comments
Forest	Forest	bestockt.geschlossener _Wald	Closed forest	Bodenbedeckung	
		bestockt.uebrige_bestockte	Mixed planted	Bodenbedeckung	Hedgerows, Planted roadsides, etc.
Intensively used open-land	No equivalent	humusiert.Gartenanlage	Garden, Parks, Playgrounds, etc.	Bodenbedeckung	Includes unclassified agricultural land see 2.4
Sand and gravel pits	No equivalent	vegetations-los.Geroell_Sand	Sand and gravel	Bodenbedeckung	Mostly found within river bed
Arable land	Arable land	humusiert.Intensivkultur. Reben	Vineyard	Bodenbedeckung	
Pastures	Pastures	humusiert.Intensivkultur _uebrige_Intensivkultur	Vineyard	Bodenbedeckung	Tree nurseries, Orchards, etc.

New class	Churko equilavent	Original class	Description	Source layer	Further comments
Arable land and pastures	Arable land and pastures	humusiert. Acker_Wiese_weide	Arable land and pastures	Bodenbedeckung	This groups was further split in arable land and pastures see 2.4

Table A.2: Table of the relative resistance of the land cover classes for each of the five study species

Relative resistance of the land cover classes					
Rank	*I. alpestris*	*B. bufo*	*E. calamita*	*H. arborea*	*R. temporaria*
1	Wetlands ()	Wetlands ()	Arable land (Frei et al. 2016; Churko et al. 2020)	Wetlands ()	Forest (Popescu et al. 2011)
2	Water conductiv ()	Water conductiv ()	Pastures (Frei et al. 2016; Churko et al. 2020)	Water conductiv ()	Wetlands (Reh et al. 1990)
3	Forest (Emaresi et al. 2011)	Forest (Janin, Léna, Ray, et al. 2009; Janin, Léna, Deblois, et al. 2012)	Wetlands (Churko et al. 2020)	Pastures (Clauzel et al. 2013)	Water conductiv (Reh et al. 1990)
4	Pastures (Schmidt et al. 2006)	Pastures (Janin, Léna, Ray, et al. 2009; Janin, Léna, Deblois, et al. 2012)	Water conductiv (Churko et al. 2020)	Arable land (Clauzel et al. 2013)	Pastures (Reh et al. 1990; Popescu et al. 2011)
5	Arable land (Schmidt et al. 2006)	Arable land (Janin, Léna, Ray, et al. 2009; Janin, Léna, Deblois, et al. 2012)	Forest (Stevens, Polus, et al. 2004; Frei et al. 2016; Churko et al. 2020)	Roads and sealed surfaces (Clauzel et al. 2013; Pellet, Guisan, et al. 2004; Pellet, Hoehn, et al. 2004)	Arable land (Reh et al. 1990; Popescu et al. 2011)

Rank	*I. alpestris*	*B. bufo*	*E. calamita*	*H. arborea*	*R. temporaria*
6	Intensively used open-land ()	Intensively used open-land (Janin, Léna, Ray, et al. 2009; Janin, Léna, Deblois, et al. 2012)	Sand and gravel pits (KARCH 2020)	Forest (Clauzel et al. 2013)	Intensively used open-land ()
7	Water barrier (Luqman et al. 2018)	Sand and gravel pits (Janin, Léna, Ray, et al. 2009; Janin, Léna, Deblois, et al. 2012)	Roads and sealed surfaces (Rowe et al. 2000)	Intensively used open-land (Clauzel et al. 2013)	Sand and gravel pits ()
8	Roads and sealed surfaces (Luqman et al. 2018; Prunier et al. 2014; Emaresi et al. 2011)	Roads and sealed surfaces (Joly et al. 2003; Janin, Léna, Ray, et al. 2009; Janin, Léna, Deblois, et al. 2012)	Intensively used open-land (Churko et al. 2020)	Sand and gravel pits ()	Roads and sealed surfaces (Reh et al. 1990)
9	Sand and gravel pits (Emaresi et al. 2011)	Water barrier ()	Water barrier (Churko et al. 2020)	Water barrier (Angelone et al. 2009; Le Lay et al. 2015)	Water barrier ()
10	Buildings	Buildings	Buildings	Buildings	Buildings

Appendix B: Sensitivity analysis

In the process of adapting the method from Shirk et al. (2010) and Finch et al. (2020), many different trials were made to improve the models and the methods. There is a lot to learn from those trials but they do not belong in the core document and will therefore be presented here.

B.1 No variable scenario

To investigate the influence of the network topology and the choice of focal nodes alone on the results, I tested a no variable scenario where all edges had the same resistance similar to the isolation by distance scenario from Shirk et al. (2010). This scenario was run in CS just like the other variables and the correlation with the abundance data was also computed. It was not possible to fully wipe the effects of the network and the focal nodes out by adjusting the input. However, they could be minimized and better understood to be able to take them into account in the interpretation of the results. The few next chapters will relate the process that lead to the final models and help understand the remaining effect.

B.1.1 Effect of the network

Initially, I started working with a network representing the cadastral map called dirichlet issued from the urban planning software UrbanBEATS(Peter M. Bach et al. 2015; Peter M. Bach et al. 2015). To create this network, imagine the cadastral map was overlapped with a regular square grid which split the polygons to reduce their maximum size. The centroids of those polygons were then used as nodes of the network and connected by edges to the neighbouring polygons similarly to what has been done for the network used in the final version of the method (see chapter 2.2.2). This is a simplification of the process to give an idea of how it was computed, for more information on the dirichlet please refer to the documentation of UrbanBEATS.

However, the polygons neighbouring roads were connected to the many lines composing the roads stretches, whereas those were often only connected to their two neighbouring polygons (one on each side of the road). This created some nodes from which left many edges connected to other rather isolated nodes in some sort of radiation patterns (Figure

B.1). When the current hit those areas, it spread out across the different edges creating a seemingly low connectivity area.

This is explained by the fact that each of those edges had a rather low importance for the connectivity of the whole network because of the many alternatives available (Brad H. McRae and Beier 2007). When attributing a resistance from the variables to the edges of the network, the effect of the variable was tangled with that of the topology of the dirichlet itself. The signal of the variable I wanted to measure was, therefore, blurred out by the noise of the dirichlet. This effect of the network topology was best illustrated with the no variable scenario as seen in Figure B.1. For this reason, I opted for a regular grid network for which each node was connected to the same number of edges of equal length. This illustrates the importance of selecting a network well suited to the purpose of the study as suggested by Godet et al. (2020).

This decision was also supported by the fact that a regular network would be composed of fewer elements and were, therefore, much quicker to compute through CS.

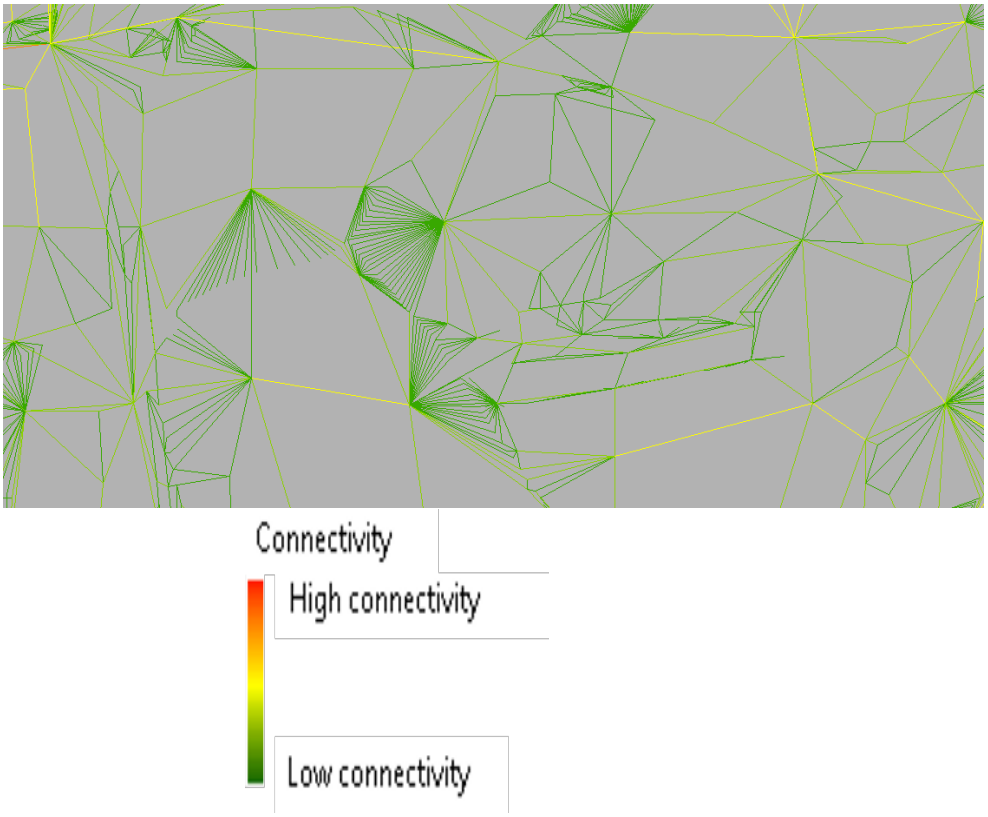

Figure B.1: Illustration of the effect of the topology of the dirichlet on the distribution of the current in the edges in the no variable scenario. The patterns of connectivity seen here are solely resulting from the network topology.

B.1.2 Effect of the focal nodes

Similarly to the topology of the network, the focal nodes had an influence on the distribution of the current in the network, as already reported by Koen, Bowman, Sadowski, et al. (2014). The current at each node was influenced by their position relative to the focal nodes (distance and centrality).

In an attempt to map the functional connectivity of the landscape, the data set of the breeding sites of national importance was first used to select the focal nodes. The nodes of the network closest to the centroids of the breeding site polygons were selected as focal nodes. The study area contained 41 focal nodes (green points in Figure B.2 (a)). It was later abandoned because the selected species did not use them equally. Some seemed to be limited to a few of the breeding sites, some were present at all of them but also at many other sites and some did not seem to rely on them at all. The data set lacked further information to attribute species to the breeding sites, the functional aspect was, therefore, only true for some of the species only. Furthermore, when using only a subsample of those breeding sites I observed substantial variation in the output correlation indicating that using the wrong breeding site for one species would induce a bias in the connectivity models and thus the resistance models.

As a result, this diversity led to a complex interpretation of the output because when running the no variable scenario, I could still observe a correlation of the current with the abundance data. This correlation was not significant for all of the species. The effect of the position of the nodes relative to the focal nodes on the correlation was, therefore, indistinguishable from that of the variables I wanted to measure.

To solve this issue I switched to the focal nodes presented in chapter 2.2.3 and resorted to model structural connectivity. Again, this illustrates the importance of making decisions according to the purpose of the study. One way to still investigate the functional connectivity would be to use suitability models to identify the focal nodes and have one set of focal nodes per species (Godet et al. 2020). This could not be done here due to lack of time.

B.1.3 Controlling for the effect of the network and the focal nodes

As mentioned above, the final network and set of focal nodes still had an effect on the diffusion of the current in the network and thus, on the correlation with the abundance data. The patterns of the no variable scenario can be seen in Figure B.2. Unexpectedly, some species still yielded significant correlation with this faint pattern but unlike with the focal nodes issued from the breeding sites the correlation was insignificant for most the species or really low (Table B.1). Most of the species presented negative correlation when the final set of focal nodes was used. *R. temporaria* stands out however with a

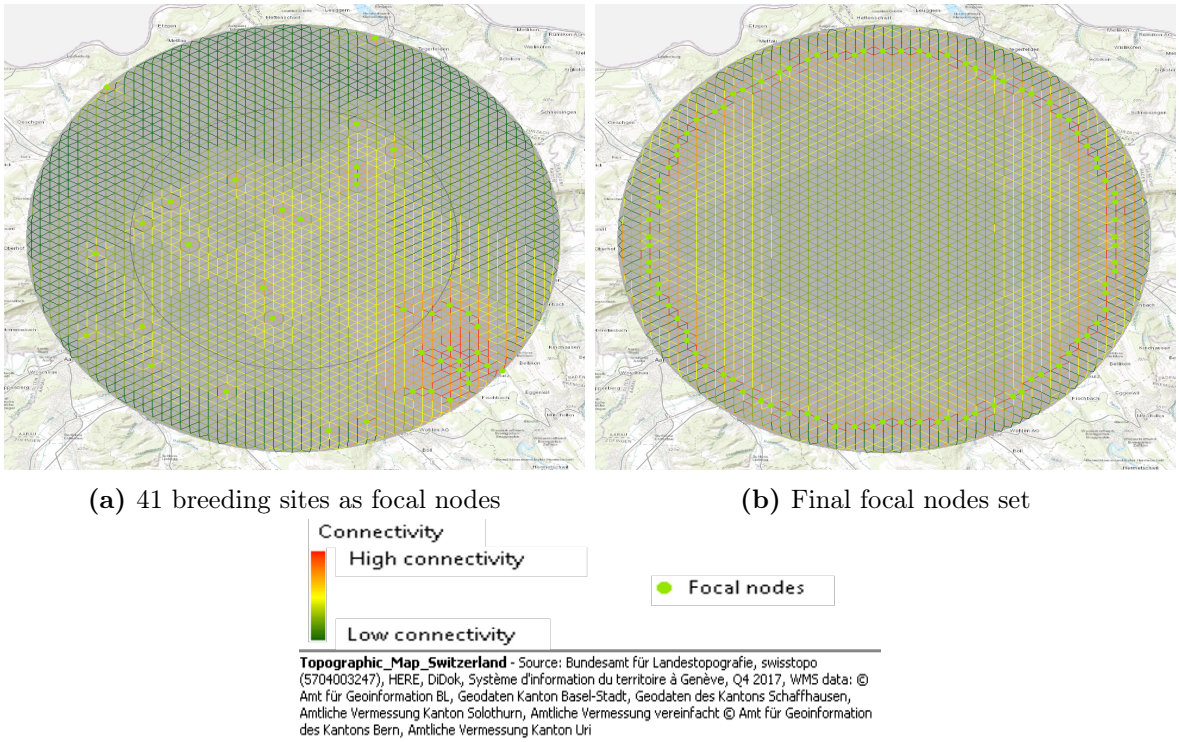

(a) 41 breeding sites as focal nodes **(b)** Final focal nodes set

Figure B.2: Current resulting from the no variable scenario for the initial focal nodes deriving from the breeding sites and the final focal nodes set around the calibration area

relatively strong significant negative correlation, it can be explained by the presence of higher observation numbers in the middle of the calibration area where the current of the no variable scenario is the lowest with the final focal nodes (Figure B.2 (b)).

Table B.1: Summary of the correlation between the current resulting from the no variable scenario and the abundance data for the two sets of focal nodes. The correlation is more uniform with the final focal nodes set and is rarely significant.

Species	Focal nodes set	Spearman's rho	S statisitc	P value
B. bufo	Breeding sites	0.1016	21791627.01	0.0198
	Final	−0.0854	28486734.35	0.0471
E. calamita	Breeding sites	0.1714	456798.99	0.0366
	Final	−0.1424	681912.98	0.0791
H. arborea	Breeding sites	0.4542	61980.66	< 0.0001
	Final	0.0736	124177.98	0.4832
I. alpestris	Breeding sites	0.0672	61982147.06	0.0684
	Final	−0.0432	73353504.48	0.2368
R. temporaria	Breeding sites	0.0565	22882484.30	0.1950
	Final	−0.1124	29194713.51	0.0089

I tried to control for this remaining impact of the network and the focal nodes by subtracting the current obtained from the no variable scenario to the resistance models of the variables. When doing this with the focal nodes issued from the breeding sites, the surface graphs of the correlation with the abundance data could vary quiet a lot

compared to the uncorrected current for some species. The ridges and peaks shifted erratically (Figure B.3 (a) and (b)). For other species it had little impact. This was not strongly related to whether the no variable scenario was significantly correlated with the abundance data of the species. Those results were, therefore, hard to interpret and contributed in the decision to switch to the final set of focal nodes. With those, the correction with the current of the no variable scenario had lower impact on the patterns of the solution space. Only the height of the ridges varied but not their location (Figure B.3 (c) and (d)). This confirmed robustness of the choice of optimum parameter sets identified and the smaller impact of the final set of focal nodes.

B.2 The number of absences

Before I set the number of absences to 1.5 times the number of presences (see chapter 2.5.2), I tested different values and observed the impact on the correlation. This was done using the most wide spread species (*I. alpestris*). The higher the number of absences was, the higher the correlation I obtained which is a sign that the results obtained were not only induced by the set of absences chosen. Furthermore, with lower numbers of absences, the correlation and the optimums varied more from one set of absences to the other similarly to what I observed in the multiple layer calibration for the rarer species (see chapter 3.4.1). I opted for this value in the end to optimize the correlation but also allow the absences set to vary slightly between the rounds for all the species. This sensitivity analysis could have been made for all the species and a unique value chosen for each of them. It was not done here due to a lack of time.

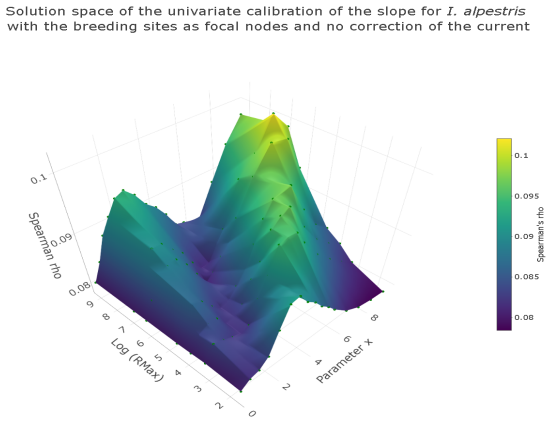

(a) 41 breeding sites as focal nodes without correction of the current

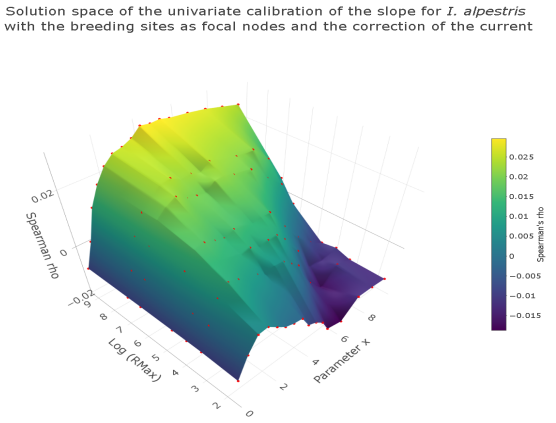

(b) 41 breeding sites as focal nodes with correction of the current

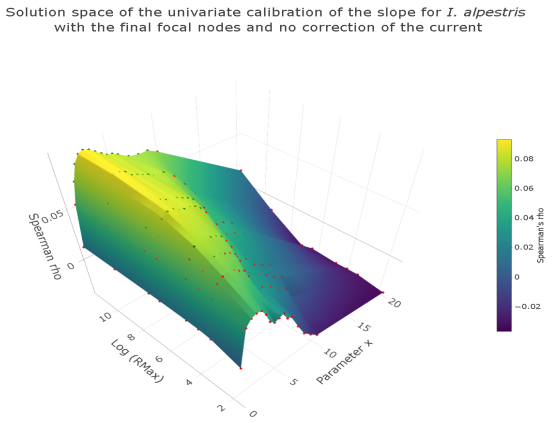

(c) Final focal nodes set without correction of the current

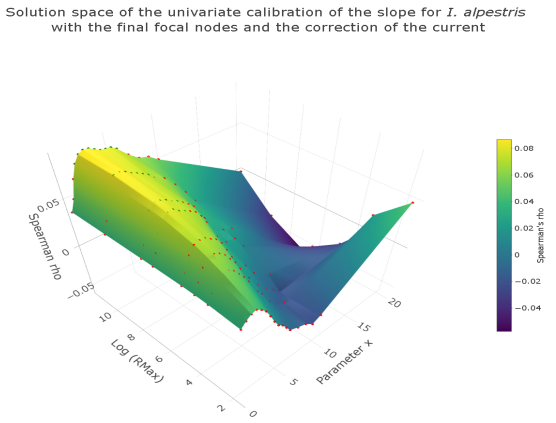

(d) Final focal nodes set with correction of the current

Figure B.3: Solution space of the univariate calibration of the variable slope for *I. alpestris* for the different focal nodes sets considered with and without the correction for the current of the no variable scenario. The parameter x is on the x-axis, the $RMax$ on the y-axis and the Spearman's rho on the z-axis. Each point on the surface is the result of one scenario (combination of parameter x and $RMax$). The color of the point indicates whether the correlation is significant or not (Green = significant, Red = not significant). The final focal nodes set is much less subject to variation when correcting for the effect of the network topology and the focal nodes.

Appendix C: Resistance and current distribution and resistance maps

This appendix details the different input of the final connectivity model. Table C.1 summarizes the distribution of the resistance in the edges for the individual resistance models of the variables and the multivariate resistance model. It also includes the distribution of the current in all of the edges resulting from the multivariate resistance model (output of the connectivity model). In a second part the maps of the resistance induced by each variable for all the species are presented. The combination of those resistance maps create those presented in Figure 4.1.

Table C.1: Summary of the distribution of the resistance and the current in the edges.

Species	Variable	Resistance/Current	Min	Max	Mean	Median	Standard deviation	Skewness
B. bufo	Shortest distance to water	Resistance	1	$1 * 10^{13}$	$2.048167 * 10^{9}$	1	$1.246044 * 10^{11}$	76.62
	Slope	Resistance	1	6	1.03	1	0.19	18.44
	Traffic	Resistance	1	501	1.82	1	13.45	24.99
	Multivariate	Resistance	3	$1 * 10^{13}$	$1.246044 * 10^{11}$	3	$1.246044 * 10^{11}$	76.62
	Multivariate	Current	0	1.3017	0.4651	0.4555	0.1612	−0.02
E. calamita	Shortest distance to water	Resistance	1	1001	1.31	1	13.78	61.54
	Slope	Resistance	1	$1 * 10^{7}$	7746.70	3.25	$1.430753 * 10^{5}$	54.60
	Traffic	Resistance	1	$1 * 10^{9}$	$6.223360 * 10^{5}$	1	$1.844070 * 10^{7}$	24.99
	Multivariate	Resistance	3	$1 * 10^{13}$	$1.246044 * 10^{11}$	3	$1.246044 * 10^{11}$	39.72
	Multivariate	Current	0	9.5667	0.6453	0.3292	0.8847	2.79
H. arborea	Shortest distance to water	Resistance	1	$1 * 10^{10}$	$4.296845 * 10^{6}$	1	$1.503678 * 10^{8}$	52.65
	Slope	Resistance	1	$1 * 10^{12}$	$3.971896 * 10^{8}$	2277.76	$1.303738 * 10^{10}$	68.17
	Traffic	Resistance	1	$1 * 10^{5}$	$2.762601 * 10^{4}$	1	$3.434517 * 10^{4}$	0.53
	Multivariate	Resistance	3	$1 * 10^{12}$	$4.015141 * 10^{8}$	$7.360320 * 10^{4}$	$1.303812 * 10^{10}$	68.16
	Multivariate	Current	0	0.1373	0.6043	0.2632	1.0148	4.13
I. alpestris	Shortest distance to water	Resistance	1	$1 * 10^{11}$	$1.003980 * 10^{8}$	1.023876	$1.925909 * 10^{9}$	35.55
	Slope	Resistance	1	$1 * 10^{5}$	4328.25	1869.38	6607.23	3.54
	Traffic	Resistance	1	$1 * 10^{6}$	$4.899605 * 10^{4}$	1	$1.163044 * 10^{5}$	4.29
	Land cover	Resistance	283.5	1063.14	639.53	626.24	122.57	0.48
	Multivariate	Resistance	412.37	$1 * 10^{11}$	$1.004520 * 10^{8}$	$1.815423 * 10^{4}$	$1.925908 * 10^{9}$	35.55
	Multivariate	Current	0	4.5066	0.5419	0.4549	0.4483	1.77
R. temporaria	Shortest distance to water	Resistance	1	$5 * 10^{4}$	$4.905551 * 10^{4}$	$4.9153 * 10$	1732.39	−26.7
	Slope	Resistance	1	$5 * 10^{6}$	5303.77	6.19	$7.567977 * 10^{4}$	47.98
	Traffic	Resistance	1	$5 * 10^{6}$	7779.84	1	$1.313722 * 10^{5}$	25.80
	Multivariate	Resistance	3	5.049611^{6}	$6.213912 * 10^{4}$	$4.932735 * 10^{4}$	$1.513889 * 10^{5}$	22.74
	Multivariate	Current	0.5354	3.1090	0.4594	0.4494	0.1487	2.30

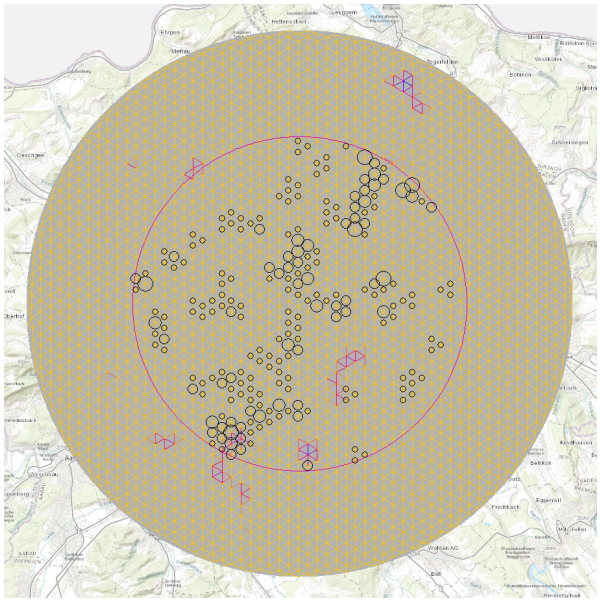

(a) Map of the resistance induced by the shortest distance to water

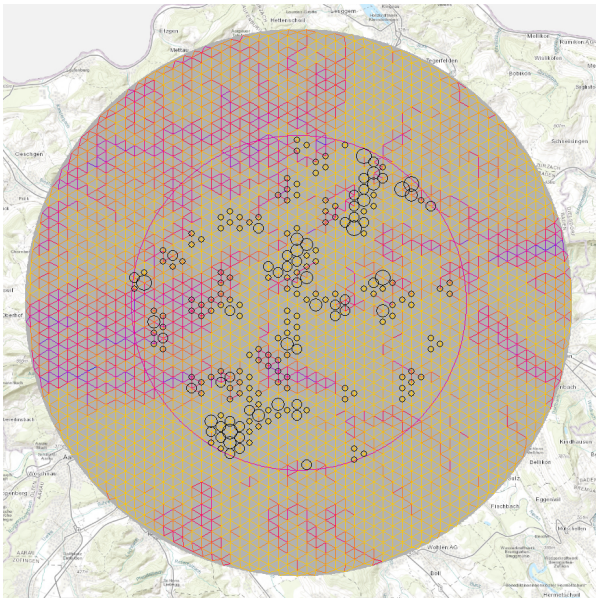

(b) Map of the resistance induced by the slope

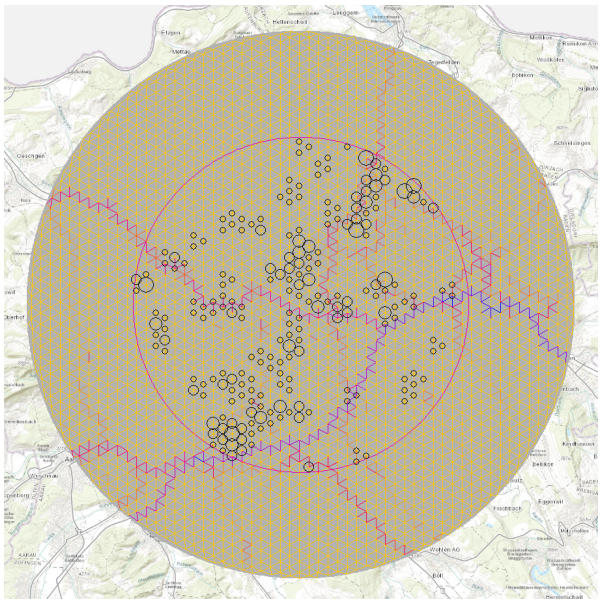

(c) Map of the resistance induced by the traffic

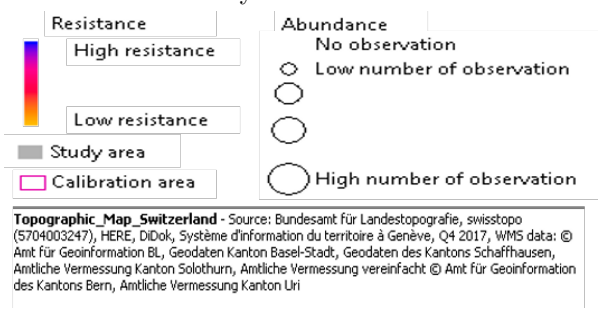

Figure C.1: Maps of the resistance induced by the optimum parameter sets identified for each of the variable included in the connectivity model of *B. bufo*. Note that the color range is specific to each variable for better representation.

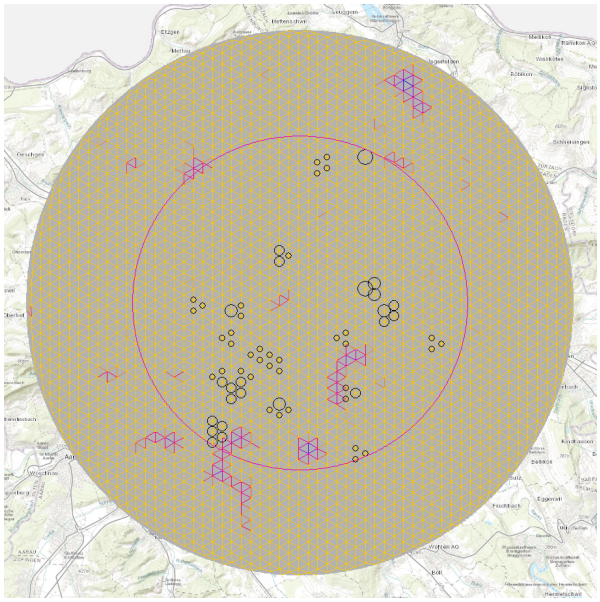

(a) Map of the resistance induced by the shortest distance to water

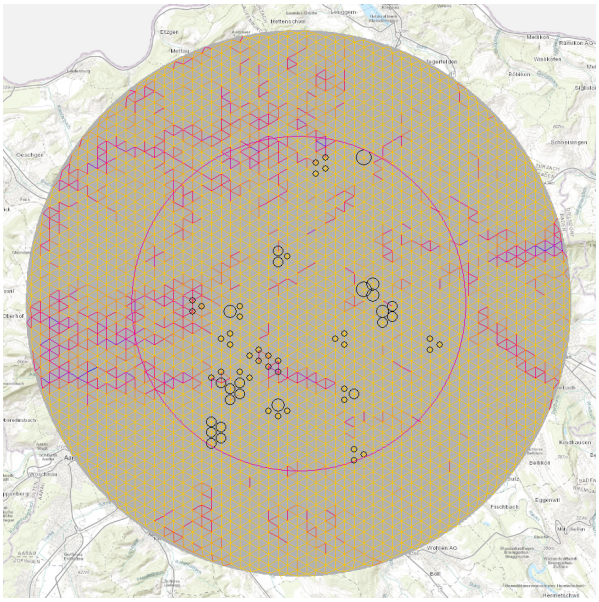

(b) Map of the resistance induced by the slope

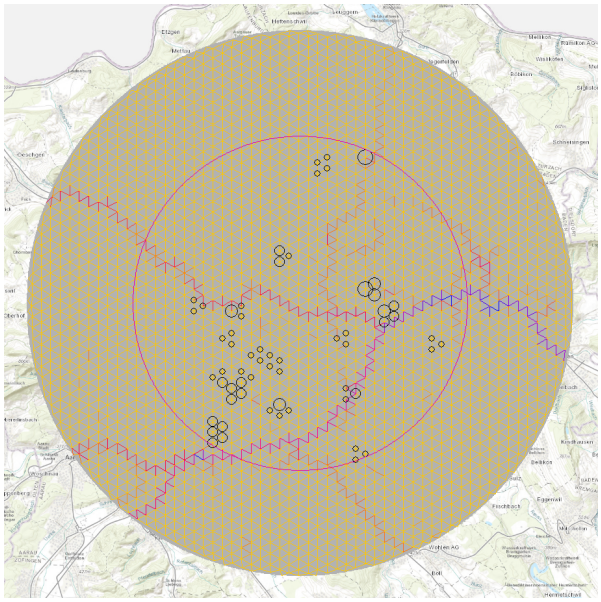

(c) Map of the resistance induced by the traffic

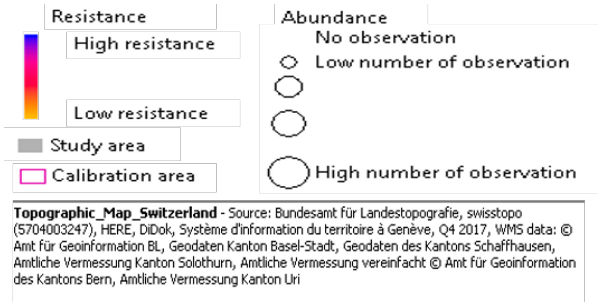

Figure C.2: Maps of the resistance induced by the optimum parameter sets identified for each of the variable included in the connectivity model of *E. calamita*. Note that the color range is specific to each variable for better representation.

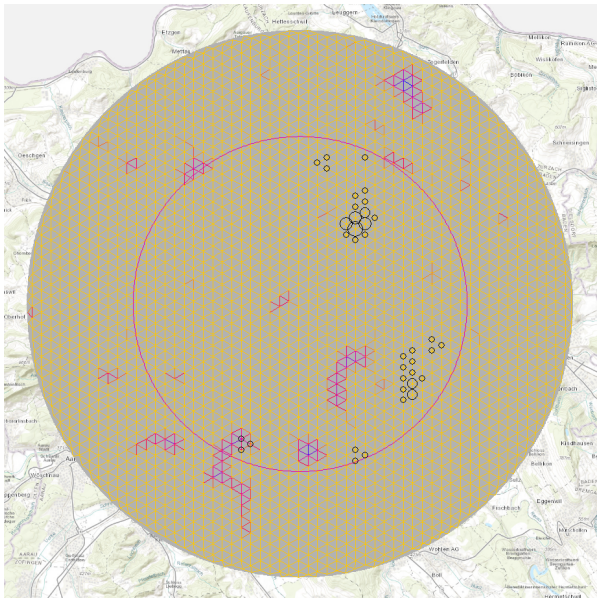

(a) Map of the resistance induced by the shortest distance to water

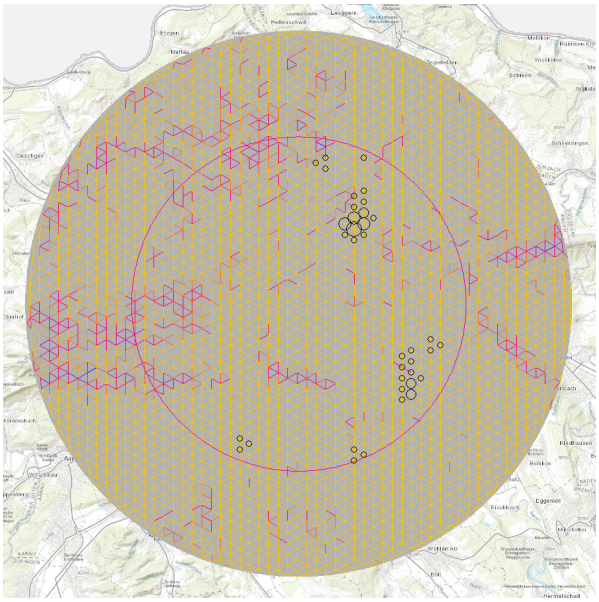

(b) Map of the resistance induced by the slope

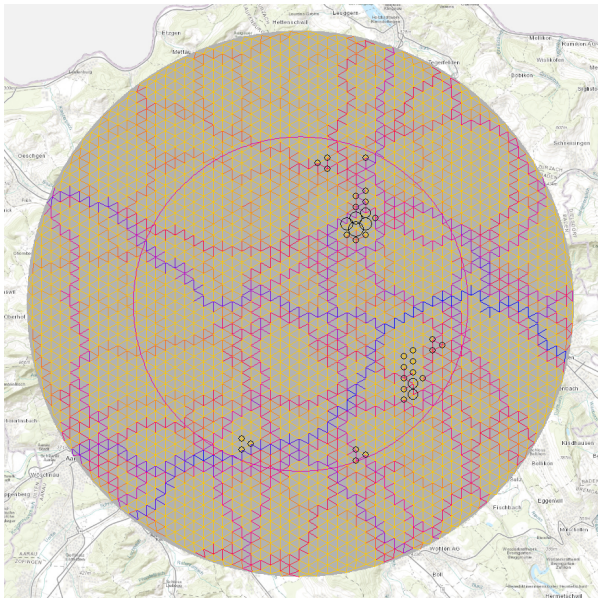

(c) Map of the resistance induced by the traffic

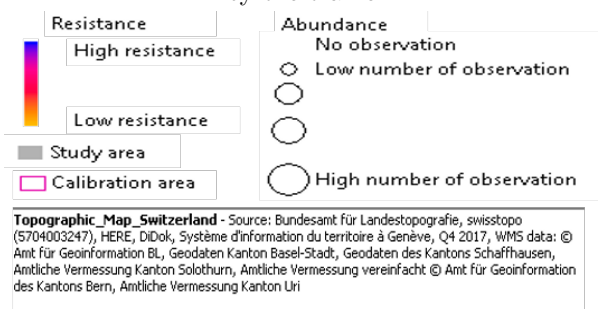

Figure C.3: Maps of the resistance induced by the optimum parameter sets identified for each of the variable included in the connectivity model of *H. arborea*. Note that the color range is specific to each variable for better representation.

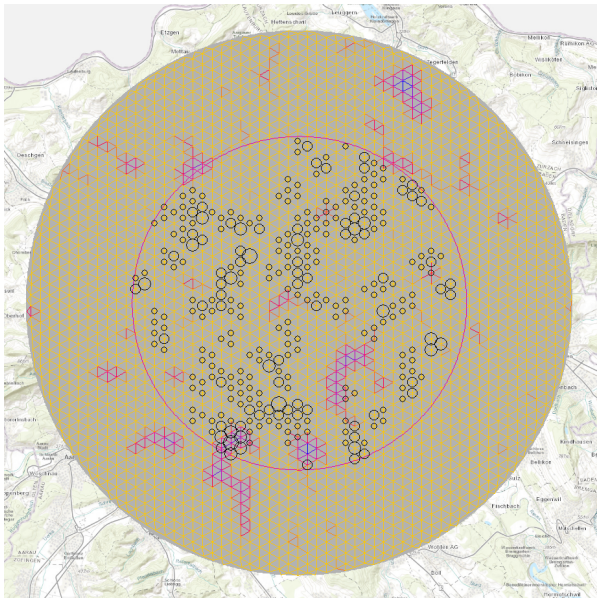

(a) Map of the resistance induced by the shortest distance to water

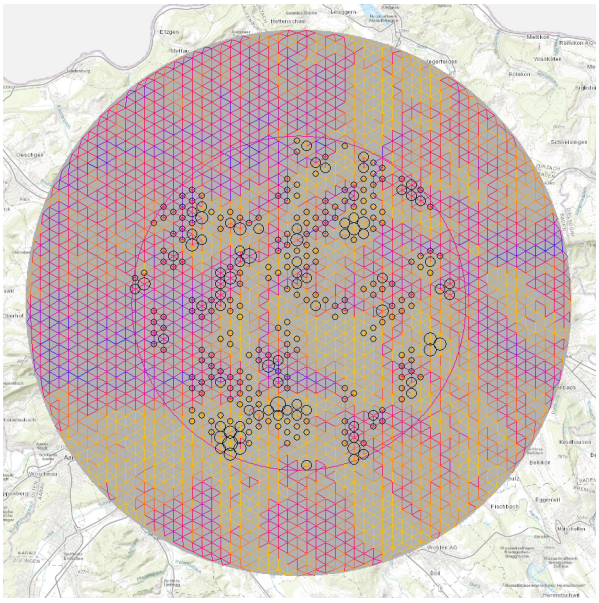

(b) Map of the resistance induced by the slope

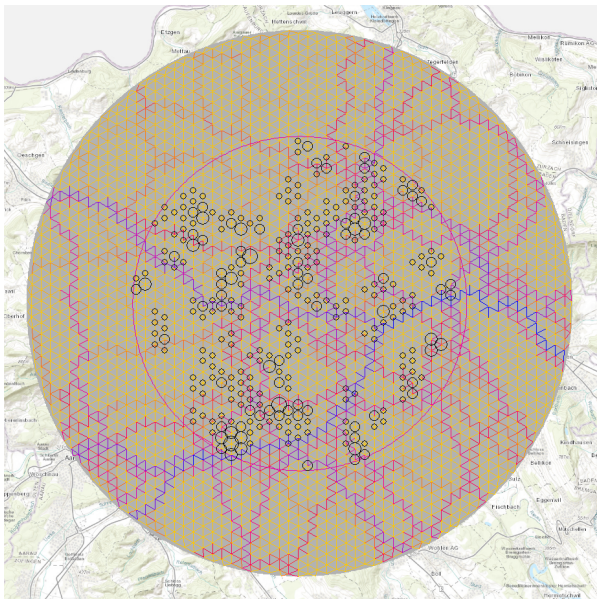

(c) Map of the resistance induced by the traffic

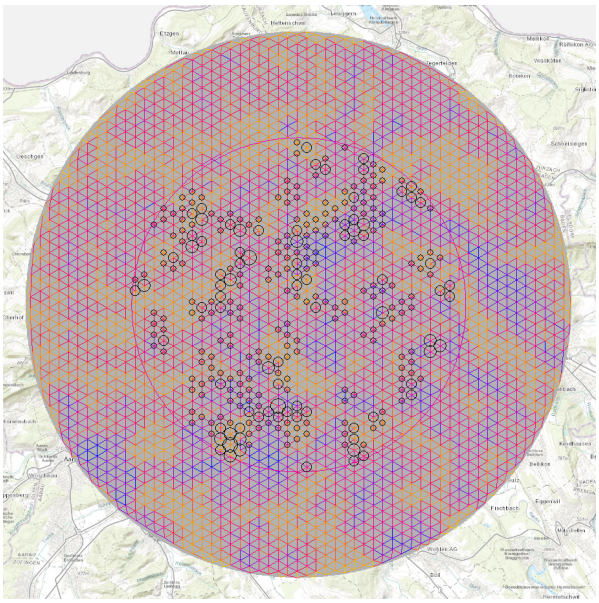

(d) Map of the resistance induced by the land cover

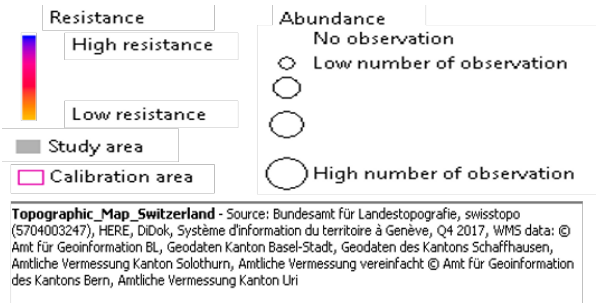

Figure C.4: Maps of the resistance induced by the optimum parameter sets identified for each of the variable included in the connectivity model of *I. alpestris*. Note that the color range is specific to each variable for better representation.

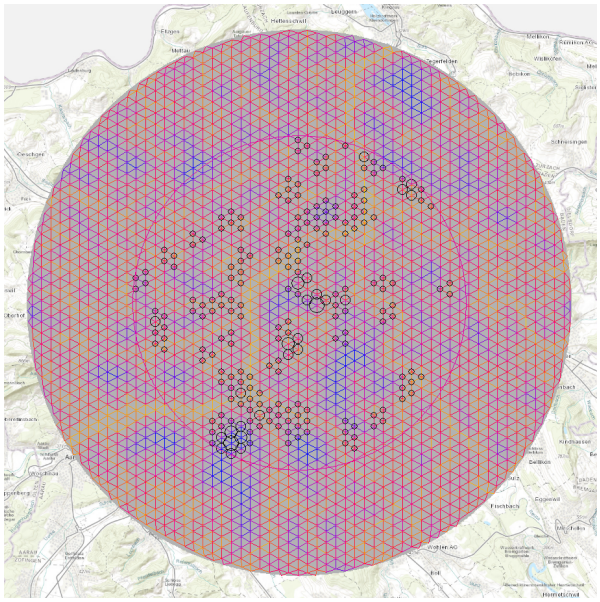

(a) Map of the resistance induced by the shortest distance to water

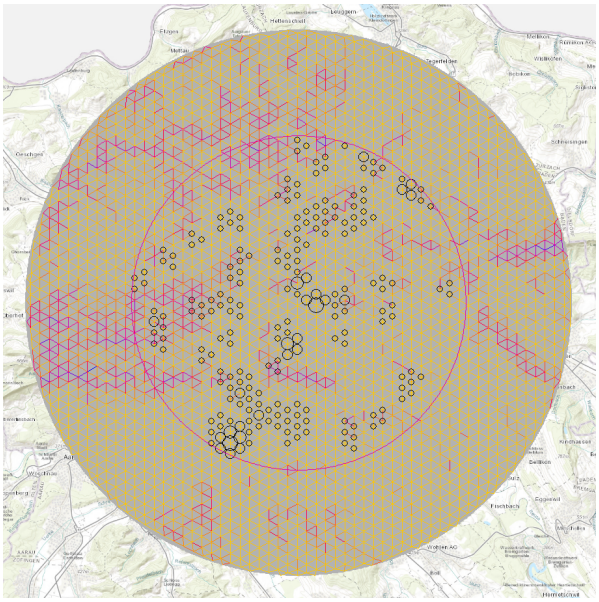

(b) Map of the resistance induced by the slope

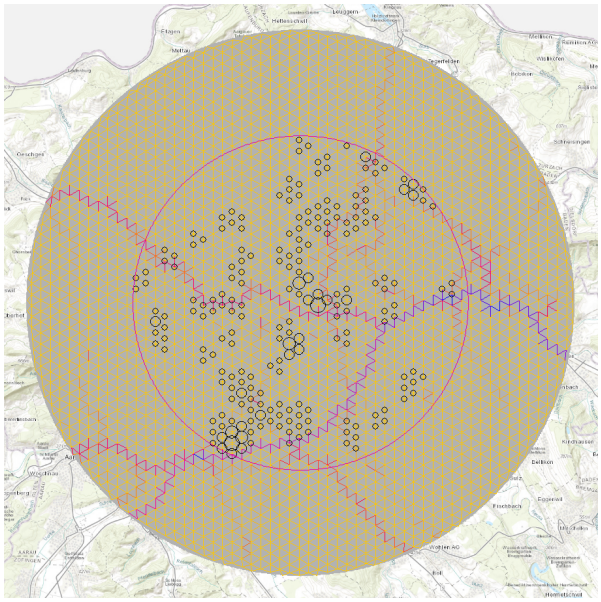

(c) Map of the resistance induced by the traffic

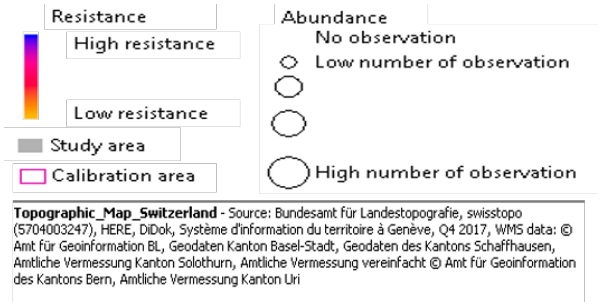

Figure C.5: Maps of the resistance induced by the optimum parameter sets identified for each of the variable included in the connectivity model of *R. temporaria*. Note that the color range is specific to each variable for better representation.

Appendix D: Declaration of originality

ETH

Eidgenössische Technische Hochschule Zürich
Swiss Federal Institute of Technology Zurich

Declaration of originality

The signed declaration of originality is a component of every semester paper, Bachelor's thesis, Master's thesis and any other degree paper undertaken during the course of studies, including the respective electronic versions.

Lecturers may also require a declaration of originality for other written papers compiled for their courses.

I hereby confirm that I am the sole author of the written work here enclosed and that I have compiled it in my own words. Parts excepted are corrections of form and content by the supervisor.

Title of work (in block letters):

INVESTIGATING LANDSCAPE RESISTANCE USING A CONNECTIVITY MODELLING METHOD

Authored by (in block letters):
For papers written by groups the names of all authors are required.

Name(s):	**First name(s):**
COTTET	ROMAIN

With my signature I confirm that
- I have committed none of the forms of plagiarism described in the 'Citation etiquette' information sheet.
- I have documented all methods, data and processes truthfully.
- I have not manipulated any data.
- I have mentioned all persons who were significant facilitators of the work.

I am aware that the work may be screened electronically for plagiarism.

Place, date	**Signature(s)**
Zürich, 06.04.2021	

For papers written by groups the names of all authors are required. Their signatures collectively guarantee the entire content of the written paper.